

E.M.F. MEASUREMENTS ON THE LIQUID
LEAD-SILVER-GOLD SYSTEM USING
A MOLTEN OXIDE ELECTROLYTE

By

Adolfo R. Zambrano

ProQuest Number: 10781632

All rights reserved

INFORMATION TO ALL USERS

The quality of this reproduction is dependent upon the quality of the copy submitted.

In the unlikely event that the author did not send a complete manuscript and there are missing pages, these will be noted. Also, if material had to be removed, a note will indicate the deletion.



ProQuest 10781632

Published by ProQuest LLC (2018). Copyright of the Dissertation is held by the Author.

All rights reserved.

This work is protected against unauthorized copying under Title 17, United States Code
Microform Edition © ProQuest LLC.

ProQuest LLC.
789 East Eisenhower Parkway
P.O. Box 1346
Ann Arbor, MI 48106 – 1346

A Thesis respectfully submitted to the Faculty and the Board of Trustees of the Colorado School of Mines in partial fulfillment of the requirements for the degree of Master of Science in Metallurgical Engineering.

Signed: Adolfo R. Zambrano
Adolfo R. Zambrano

Golden, Colorado

Date: July 31, 1968

Approved: John P. Hager
John P. Hager
(Thesis Advisor)

Albert W. Schlechten
Albert W. Schlechten
(Head, Department of
Metallurgical Engineering)

Golden, Colorado

Date: July 31, 1968

ABSTRACT

The thermodynamic properties of the liquid Pb-Ag-Au system have been determined from galvanic cell measurements for five pseudo-binaries of fixed $X_{\text{Ag}}/X_{\text{Au}}$ ratios. The galvanic cell employed a molten PbO-SiO₂ electrolyte saturated with silica in the temperature range from 775-1030^oC.

The thermodynamic properties of Pb were calculated at 1200^oK directly from the e.m.f. measurements, whereas the properties of Ag and Au were obtained by means of the Gibbs-Duhem integration.

No anomalies could be detected in the ternary field, and the calculated properties of the Ag-Au system agree well with the published properties.

CONTENTS

	Page
ABSTRACT	iii
CONTENTS	iv
LIST OF FIGURES	vi
LIST OF TABLES	ix
LIST OF APPENDICES	x
ACKNOWLEDGMENTS	xi
I. INTRODUCTION	1
A. The galvanic Cell Technique	1
B. Outline of this Study	3
II. LITERATURE SURVEY	8
A. The Lead Oxide-Silica System	8
B. The Lead-Silver System	8
C. The Lead-Gold System	12
D. The Silver-Gold System	16
III. APPARATUS AND EXPERIMENTAL PROCEDURE	21
A. Description of the Apparatus	21
B. Experimental Procedures	25
IV. REDUCTION OF THE EXPERIMENTAL DATA	28
A. Thermodynamic Computations	28

CONTENTS(continued)

B. Estimation of Uncertainties	34
C. Use of the Computer	36
V. RESULTS	38
A. E.m.f. Measurements on the Lead-Silver-Gold System	38
B. Calculations of the Thermodynamic Properties for the Lead-Silver-Gold System	38
VI. DISCUSSION	59
A. Estimation of the Thermodynamic Properties for the Silver-Gold System	59
B. Thermodynamic Data Compared to Current Solutions Models	63
VII. SUMMARY AND CONCLUSIONS	66
VIII. SUGGESTIONS FOR FURTHER WORK	67
APPENDICES	70
LITERATURE CITED	91
BIOGRAPHICAL NOTE	95

LIST OF FIGURES

<u>Figure</u>		<u>Page</u>
1.	The Lead Oxide-Silica Equilibrium Diagram.	9
2.	The Lead-Silver Equilibrium Diagram.	11
3.	The Lead-Gold Equilibrium Diagram.	15
4.	The Silver-Gold Equilibrium Diagram.	18
5.	Activities of Silver and of Gold in their Liquid Alloys, Relative to the Pure Liquids.	20
6.	Galvanic Cell Design.	22
7.	Schematic View of the Equipment Arrangement.	23
8A.	Experimental Data.	42
8B.	Experimental Data.	43
8C.	Experimental Data.	44
8D.	Experimental Data.	45
8E.	Experimental Data.	46
9a.	Isoactivity Lines for Lead in the Liquid Pb-Ag-Au System at 1200 ^o K.	50
9b.	Activity of Lead in the Liquid Pb-Ag-Au System at 1200 ^o K.	51

LIST OF FIGURES(continued)

<u>Figure</u>		<u>Page</u>
10.	G^E of Liquid Pb-Ag-Au Alloys at 1200 ^o K.	52
11.	H^M of Liquid Pb-Ag-Au Alloys at 1200 ^o K.	53
12.	Isoactivity Lines for Silver in the Liquid Pb-Ag-Au System at 1200 ^o K.	54
13.	Isoactivity Lines for Gold in the Liquid Pb-Ag-Au System at 1200 ^o K.	55
14.	TS^E of Liquid Pb-Ag-Au Alloys at 1200 ^o K.	56
15.	Alpha Functions of Lead at 1200 ^o K in the Liquid Pb-Ag-Au System.	57
16.	Alpha Functions of Lead in Liquid Pb-Ag-Au Alloys at Constant Mole Fractions of Lead at 1200 ^o K.	58
17.	Pseudo-binaries Selected to Calculate the Thermodynamic Properties of the Pb-Ag-Au System.	60
18.	Activities of Silver and Gold in the Liquid Ag-Au System at 1200 ^o K.	61
19.	Excess Integral Molar Properties of the Liquid Ag-Au System at 1200 ^o K.	62
20.	Alpha Function of Silver in Liquid Ag-Au Alloys at 1200 ^o K by Integration from the Ternary Field.	65

LIST OF FIGURES(continued)

<u>Figure</u>	<u>Page</u>
app C. Calibration of Thermocouple.	73
app E. Temperature Profile of the Metal and Electrolyte inside the Galvanic Cell.	76

LIST OF TABLES

<u>Table</u>		<u>Page</u>
1.	Smooth Values of the Thermodynamic Properties of the Liquid Lead-Silver System at 1200 ^o K. ⁽⁴⁾	13
2.	Smooth Values of the Thermodynamic Properties of the Liquid Lead-Gold System at 1200 ^o K. ⁽⁵⁾	17
3.	Thermodynamic Properties of Liquid Ag-Au Alloys at 1200 ^o K, according to Hultgren <u>et al</u> ²² .	19
4.	Experimental Data for Liquid Pb-Ag-Au Alloys.	39
5.	Smooth Values of the Alpha Functions at 1200 ^o K.	47
6.	Smooth Values of the Beta Functions at 1200 ^o K.	48
7.	Chemical Analysis of Knowns.	79
8.	Chemical Analysis of Alloys.	80

LIST OF APPENDICES

<u>Appendix</u>		<u>Page</u>
A.	Experimental Data for Liquid Pb-Ag Alloys ⁴ .	71
B.	Experimental Data for Liquid Pb-Au Alloys ⁵ .	72
C.	Calibration of Thermocouple.	73
D.	Chemical Analysis of Materials.	74
E.	Temperature Profile of the Metal and Electrolyte inside the Galvanic Cell.	76
F.	Atomic-Absorption Analysis of Lead and Gold in Pb-Ag-Au Alloys.	77
G.	Experimental Data for the Pb-Ag-Au System.	83

ACKNOWLEDGMENTS

The author wishes to express his sincere appreciation to Professor John P. Hager for his guidance and continuous encouragement throughout this study.

Special thanks are also extended to Dr. Albert W. Schlechten and the Institute of Extractive Metallurgy for providing a portion of the funds to construct the experimental apparatus.

The following institutions are also gratefully acknowledged:

The Colorado School of Mines Foundation, Inc., for the financial support under Research Project Grant No. F6619.

The Kennecott Copper Corp. for providing the gold necessary to accomplish this study.

The Universidad Nacional de Colombia and the Ministerio de Minas de Colombia, South America, for providing me the economical support needed for attending the Colorado School of Mines.

I. INTRODUCTION

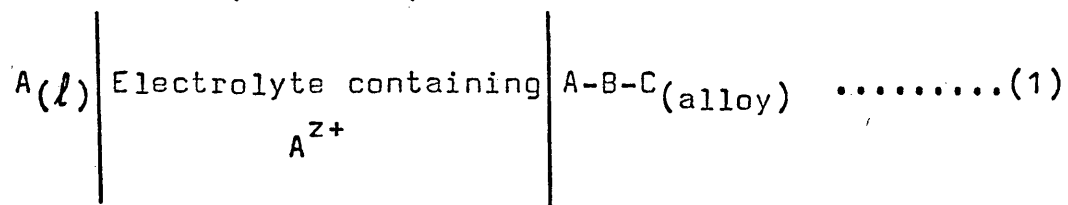
In this study, the thermodynamic properties of the liquid lead-silver-gold system are determined by means of the galvanic cell technique using a molten oxide electrolyte.

It is believed that this study will provide more data upon which the structure of metallic solutions, the prediction of compatibility of materials, and behavior of high temperature processes can be better understood.

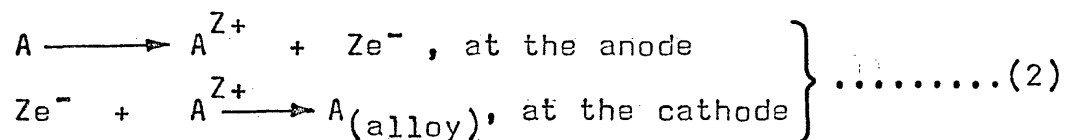
A. The Galvanic Cell Technique

To investigate the thermodynamic properties of alloys, one of the most profitable techniques is by e.m.f. measurements on a high temperature concentration cell.

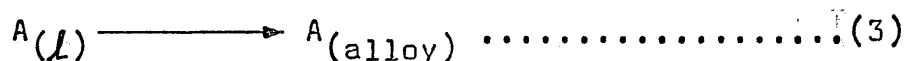
To accomplish the e.m.f. measurements, the more electro-positive component A of the alloy is used as the anode, an alloy of A is used as the cathode, and an electrolyte containing ions of A is used to provide the bridge between the two electrodes, that is,



For this particular cell, the half reactions are:



The overall reaction for the passage of Z faradays of positive electricity from left to right is:



The corresponding free energy change in the cell for this reaction is:

$$\Delta G = - ZFE \dots\dots\dots(4)$$

where,

ΔG = the Gibbs free energy change for reaction (3).

E = the e.m.f. of the cell in volts.

Z = the valence of A in the electrolyte.

F = the Faraday constant.

Further, the ΔG for reaction (3) may be expanded in the following form:

$$\Delta G = \Delta G^{\circ} + RT \ln(a_A)$$

If pure liquid A is chosen as the standard state of A in the alloy, then $\Delta G^{\circ} = 0$.

Accordingly,

$$\Delta G = RT \ln(a_A) = G_A^M = - ZFE \dots\dots\dots(5)$$

where,

G_A^M = the partial molar free energy of mixing of A in the alloy.

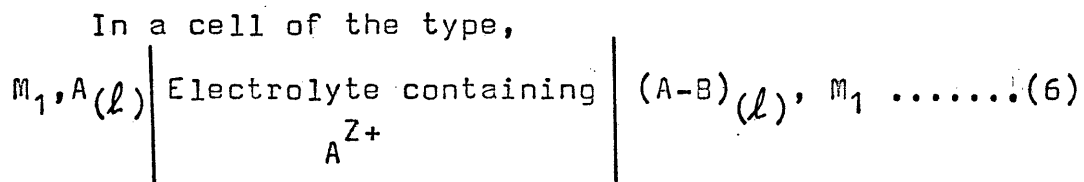
a_A = the Raoultian activity of A in the alloy.

Since the e.m.f. can be determined with high precision, the free energy change for $A(l)$ going into solution in the alloy can also be precisely determined. However, the limitations of this technique should be evaluated very carefully to guarantee its applicability to the system at hand.

B. Outline of this Study

The use of a concentration cell between a pure metal and alloys of that metal to determine the thermodynamic properties of metallic solutions was first introduced by Taylor¹. Since then, the thermodynamic properties of many alloy systems have been successfully studied by this technique, Chipman, Elliott, and Averbach².

a) Analysis of the Limitations of Galvanic Cells. Precise e.m.f. measurements obtained by the galvanic cell technique do not necessarily imply high accuracy. To add this second desirable condition, it is necessary to analyze the possible systematic errors in the system.



where,

A = the more electro-positive metal,

M_1 = the lead wires, and

(A-B) = the alloy of A with B,

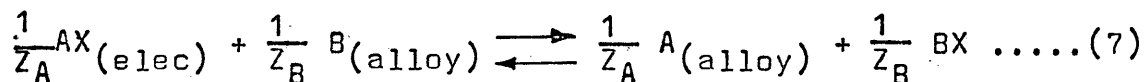
it is possible to have reactions in addition to those indicated in (2) which result in serious systematic errors in the observed e.m.f. To reduce the interferences to a minimum, the following conditions should be met:

1. The electrolyte should possess only ionic conductivity because the presence of any electronic conductivity will result in a lower e.m.f. due to the transport of electrons through the electrolyte. The value of Z will therefore be greater than the valence state of the transported ion in the electrolyte.

2. The ions of A must be present in only one state of oxidation so that the value of Z will be uniquely defined.

3. No reactions should occur between the electrolyte and the contact leads, the crucible materials, or the cell atmosphere. Any of these reactions may result in an alteration of the electrolyte or electrodes, or both.

4. Displacement reactions must be kept at a minimum.



This reaction which occurs at the electrolyte-alloy interface increases the concentration of A at the alloy electrode making the alloy interface composition different than the analyzed bulk concentration.

Wagner and Werner³ have shown that the percentage error

in the activity of A due to the displacement reaction can be calculated from the expression:

$$\epsilon = (K/X_A) \times 100 \dots\dots\dots(8)$$

where,

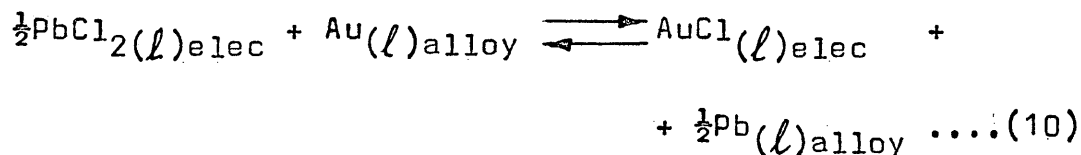
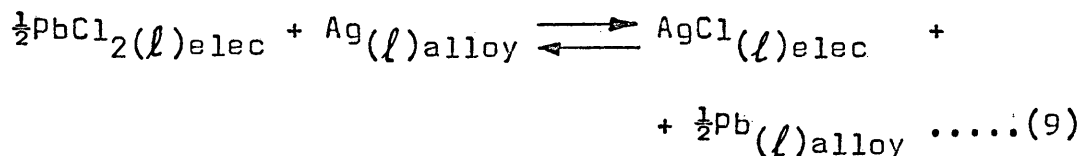
K = the equilibrium constant for reaction (7)

X_A = the mole fraction of A in the alloy

ϵ = the percentage error in the activity of A.

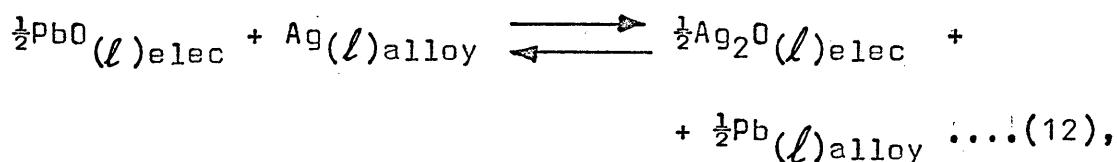
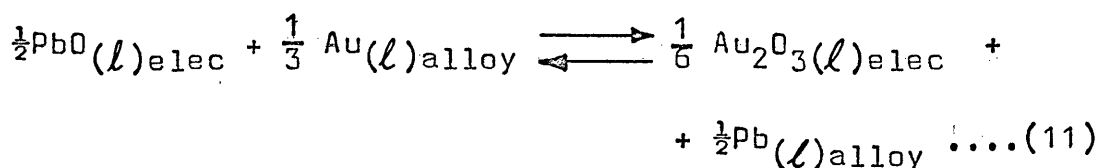
A free energy change of +7000 calories or greater for reaction (7) is necessary to expect an error in the calculated activity of A of less than 10% for an alloy containing 10 mole-% of A

b) The Galvanic Cell used in this Study. The use of conventional mixtures of alkaline chlorides containing $PbCl_2$ can give erroneous e.m.f. measurements due to the following displacement reactions:



These two reactions do not have sufficiently large positive changes in free energy to assure accurate e.m.f. measurements on galvanic cells utilizing a molten salt electrolyte containing $PbCl_2$.

For the reactions,



the following estimates of error in the activity of lead have been made:

1) Hager and Wilkomirsky⁴ have calculated the error in the a_{Pb} for Pb-Ag alloys with the following result:

at 1000°C and $X_{\text{Pb}} = 0.1$,

$$\epsilon = 0.3\%$$

2) Hager and Walker⁵ have estimated the ΔG_f^0 of Au_2O from measurements on a cell of type (6) where pure liquid Au substituted the alloy. From these measurements the error in the a_{Pb} for Pb-Au alloys was calculated as follows:

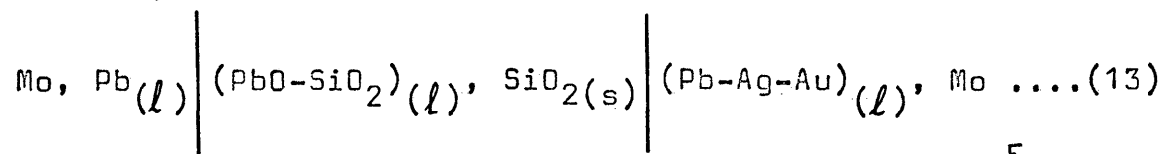
at 1075°C and $X_{\text{Pb}} = 0.01$,

$$\epsilon = 0.2\%$$

The works of Hager and Wilkomirsky⁴, and Hager and Walker⁵ have shown that the molten oxide electrolyte is a more suitable electrolyte than the conventional mixture of alkaline chlorides.

Based in part on these two preceding studies, the present study is concerned with:

a) The determination of the thermodynamic properties of liquid lead-silver-gold alloys using PbO-SiO_2 melts as the electrolyte for the following cell:



b) The estimation of activities of Ag and Au, G^E , and H^M in the liquid Ag-Au system based upon the e.m.f. measurements in the ternary system.

II. LITERATURE SURVEY

A. The Lead Oxide - Silica System.

The equilibrium phase diagram has been established by Krakau and Vakhramer⁶; Geller, Creamer, and Bunting⁷; and Krakau, Mukhin, and Heinrich⁸ (see Fig. 1).

The rate of evaporation of PbO was measured by Preston and Turner⁹ by the Vapor Pressure method and from these data Callow¹⁰ attempted to calculate the activities of PbO. Heats of formation of PbO-SiO₂ mixtures were determined at room temperature by Shartis and Newman¹¹, and finally, activities of PbO in SiO₂ melts have been also investigated by Richardson and Webb¹², and Ito and Yanagese¹³.

Concerning the transport characteristics of PbO and PbO-SiO₂, Bockris and Kitchener¹⁴, and Bockris and Mellors¹⁵ have shown that in the liquid state these compounds are essentially ionic conductors. The same conclusion was reached both by Hager and Wilkomirsky⁴, and Hager and Walker⁵.

B. The Lead - Silver System.

The phase diagram is well established in its entire composition. This system presents an eutectic at 304°C and

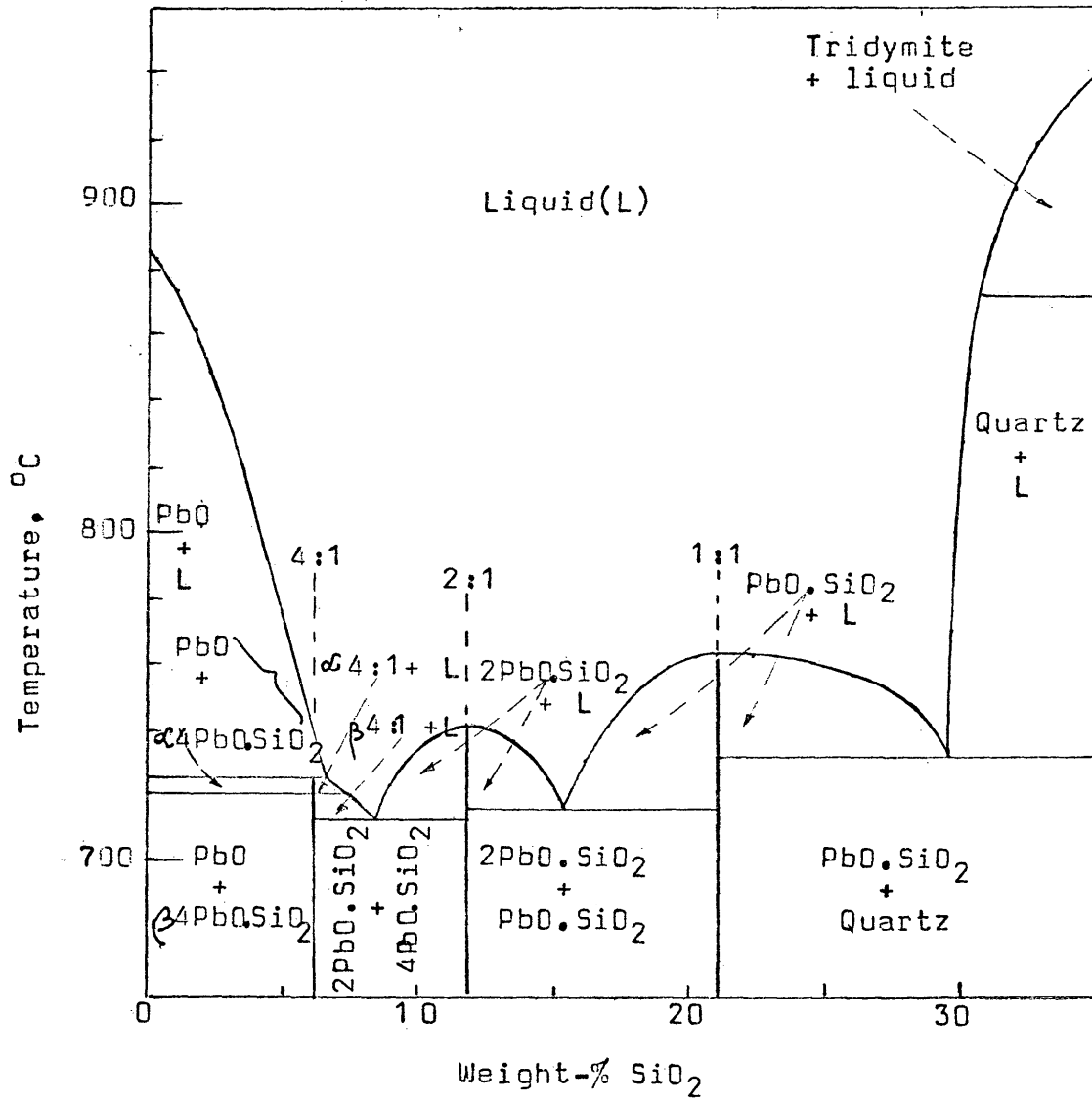


Fig. 1. The lead oxide-silica equilibrium diagram.

95.3 atomic-% of lead (see Fig. 2). The solid solubility of lead in silver is 2.0 wt-% at 900°C, and the solid solubility of silver in lead is less than 0.07 wt-% at about 200°C, (Hansen¹⁶).

Heats of mixing obtained by calorimetric techniques are not in good agreement. Kawakami¹⁷ measured positive heats of mixing at 1323°K, and Von Samson-Himmelstjerna¹⁸ in the temperature range from 293 - 1273°K estimated smaller positive heats of formation than Kawakami. For alloys of less than 10 atomic-% silver, Kleppa¹⁹ measured the heats of formation at 273°K, and the heats of formation for the entire range of composition and from 577 - 1250°K were investigated by Orr and Sommelet²⁰. The heats of mixing obtained by Hager and Wilkomirsky⁴ by galvanic cell technique agree well with other investigators^{18,20}, and represent a very good compromise for the available data on heats of mixing.

Direct determination of activities by Vapor Pressure methods have been also used. Granovskaya and Liubimov²¹ using an effusion tracer technique studied the entire composition range of lead, but their results were found by Hultgren et al²² not to conform to the Gibbs-Duhem relationship. Aldred and Pratt²³ by a torsion-effusion technique covered the range from 0.1 - 0.9 mole fraction of lead from 900 - 1080°K; unfortunately their results do not agree with those of other investigators.

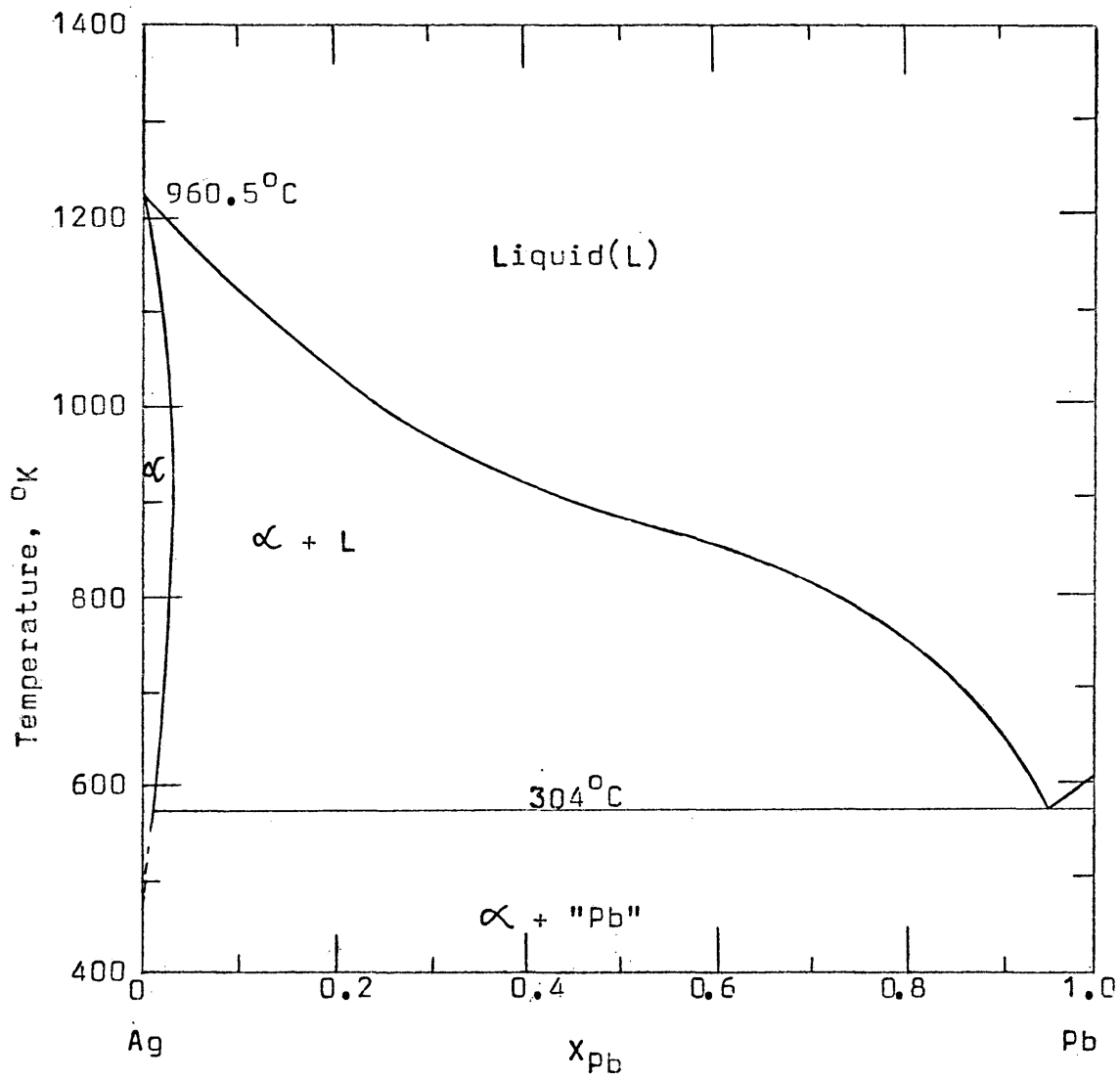


Fig. 2. The lead-silver equilibrium diagram.

Finally, galvanic cell studies reporting excellent results have completely defined the thermodynamic properties of the lead-silver system. Terpilowski²⁴, using chloride as the electrolyte, studied the range of mole fraction of lead from 0.05 to 0.93 at temperatures going from 773 - 1273^oK, and Eremenko²⁵ studied the range of composition from 0.44 - 0.91 mole fraction of lead from 720 - 1050^oC. The results of these two studies agree well with each other, and for mole fractions of lead above 0.4 these results are also in reasonable agreement with the phase diagram calculations of Hultgren et al²². Kubaschewski and Catterall²⁶ have estimated some thermodynamic properties for the lead-silver system from the equilibrium diagram and the experimental results of other investigators^{24,25}, but these calculations do not show agreement at all. The experimental results obtained by Hager and Wilkomirsky⁴, which offer the most accurate set of data on activities in the Pb-Ag system, will be used in this study to perform the Gibbs-Duhem integration in the ternary field. Smooth values of the thermodynamic properties used in this study are given in Table 1 and their experimental results are presented in Appendix A.

C. The Lead - Gold System.

The phase diagram by Hansen¹⁶ is based mainly on the work of Vogel²⁷. Two intermediate phases, Au₂Pb and AuPb₂, exist, Au₂Pb seeming to be unstable at low temperatures. The

TABLE 1. Smooth Values of the Thermodynamic Properties
of the Liquid Lead-Silver System at 1200°K⁽⁴⁾.

X_{Pb}	a_{Pb}	a_{Ag}	α_{Pb}^*	β_{Pb}^*	TS^E
0.0	0.0	1.000			0
0.1	0.153	0.899	1250	2730	125
0.2	0.300	0.798	1500	3280	242
0.3	0.430	0.694	1750	3840	350
0.4	0.541	0.633	2000	4200	424
0.5	0.623	0.561	2100	4400	460
0.6	0.686	0.491	2080	4600	475
0.7	0.757	0.413	2060	4830	430
0.8	0.828	0.320	2040	5380	340
0.9	0.907	0.193	2020	6200	210
1.0	1.000	0.0			0

* Values of α_{Pb} , β_{Pb} , and TS^E are given in cal/gfw.

solid solubility of Au in Pb is 0.076 wt-% at 200°C. The solubility of Pb in Au was found to be 0.01 wt-% between 950° and 700°C, and 0.05- to 0.04 wt-% from 600° to 500°C (see Fig. 3). Finally, part of the liquidus line was recently redefined by Hager and Walker⁵.

The heat contents of liquid and solid alloys above room temperature were first measured by Kubaschewski²⁸ for $X_{Pb} = 0.667$ and at temperatures from 440° to 800°K. His results indicate a $C_p = 2.0$ cal/(deg.gm-atom) for the liquid between 600° and 720°K. However, according to Hultgren et al²², these data are not of high precision.

By calorimetric techniques also, Kleppa¹⁹ measured the heat contents of liquid alloys for mole fractions of lead from 0.67 to 0.98 at 723°K. His results indicate a $C_p = 3.2 \pm 0.5$ cal/(deg.gm-atom) for the liquid alloys. These two works do not present any agreement. Therefore, it seems that the only reliable data on heats of mixing are those obtained by Hager and Walker⁵.

E.m.f. measurements have been also reported for liquid alloys. Kleppa²⁹ studied eighteen compositions between 723° and 1073°K. According to Hultgren et al²², Kleppa's results²⁹ seem to be established with reasonable precision.

The experimental results obtained by Hager and Walker⁵ for the entire range of composition, represent the best piece

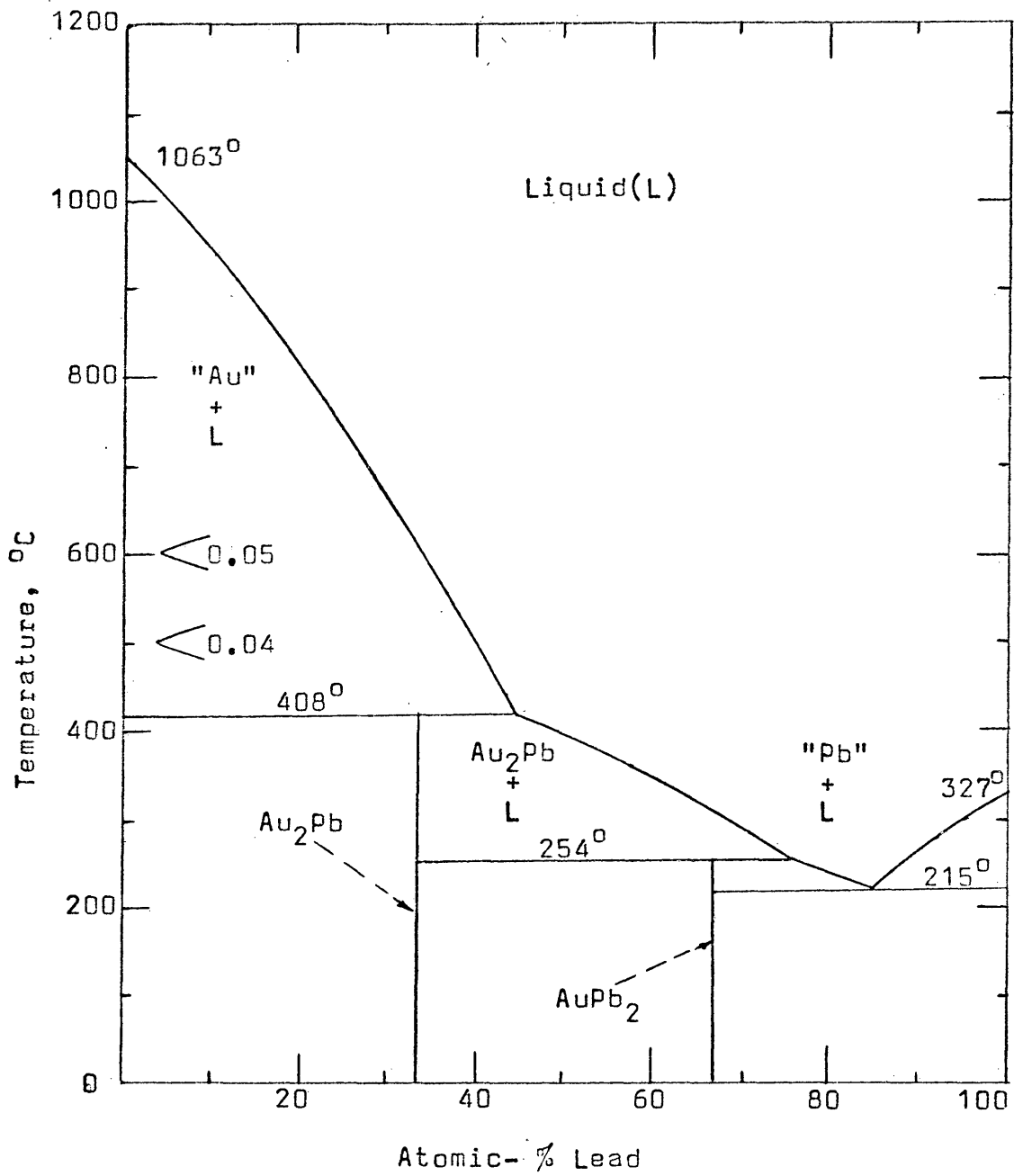


Fig. 3. The lead-gold equilibrium diagram.

of data on activities for the Pb-Au system. Their results will be used in this study to perform the Gibbs-Duhem integration in the ternary field. Smooth values of the thermodynamic properties used in this study are given in Table 2 and their experimental results are presented in Appendix B.

D. The Silver - Gold System.

In the phase diagram by Hansen¹⁶, the liquidus and solidus curves are due to Janecke³⁰ and Raydt³¹. The assumption that the system consists of a continuous series of solid solutions with no formation of ordered structures at temperatures between the solidus and room temperature has been confirmed by studies of physical properties. However, anomalies in thermodynamic properties such as activity coefficient have been considered compatible with the existence of intermediate phases or ordered structures. The parameter vs. composition curve shows a minimum close to 50 atomic-% Au, but no superstructures could be detected by Wagner³² in alloys of compositions Ag_3Au , AgAu , and AgAu_3 ; however, he did find evidence for a partial ordering of the atoms in the 50 atomic-% alloy (see Fig. 4).

E.m.f. measurements have provided the available data on liquid alloys. Wagner and Engelhardt³³ reported activities of silver at 1085°C , and Oriani³⁴ determined activities of silver and gold at 1071°C for a narrower range of composition

TABLE 2. Smooth Values of the Thermodynamic Properties
of the Liquid Lead-Gold System at 1200°K⁽⁵⁾.

x_{Pb}	a_{Pb}	a_{Au}	α_{Pb}^*	β_{Pb}^*	TS^E_*
0.0	0.000	1.000			0
0.1	0.035	0.884	-2960	-930	185
0.2	0.094	0.746	-2670	-810	302
0.3	0.177	0.605	-2430	-760	400
0.4	0.278	0.474	-2250	-650	440
0.5	0.391	0.360	-2210	-250	452
0.6	0.508	0.261	-2330	+450	446
0.7	0.631	0.174	-2610	1240	408
0.8	0.759	0.100	-3030	2100	326
0.9	0.887	0.049	-3490	3180	193
1.0	1.000	0.000			0

* Values of α_{Pb} , β_{Pb} , and TS^E are given in cal/gfw.

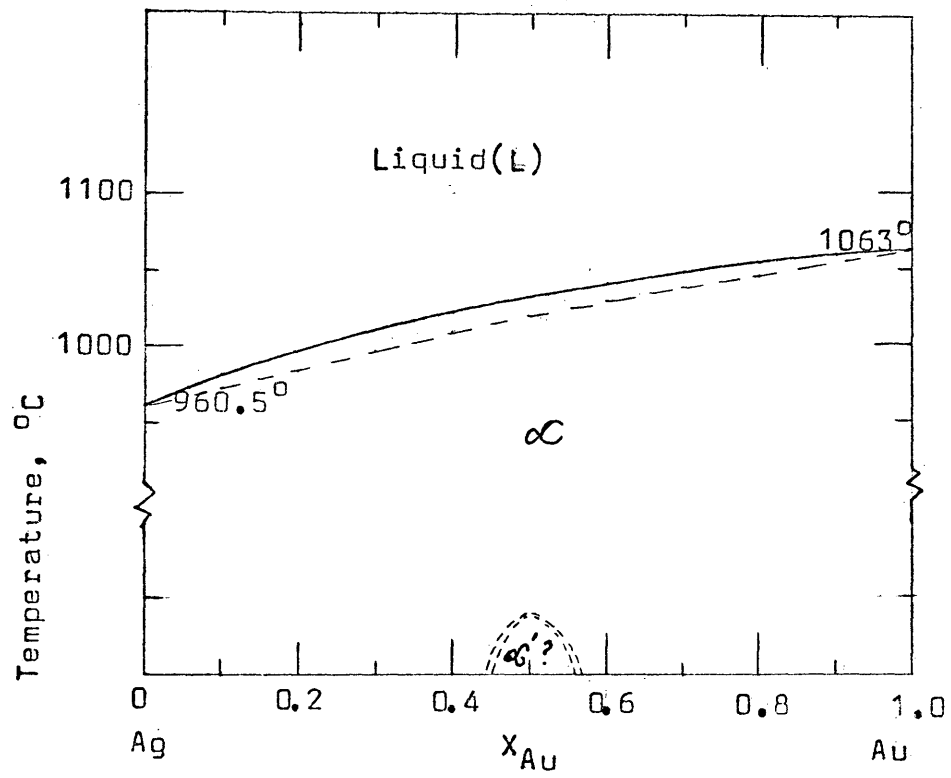


Fig. 4. The silver-gold equilibrium diagram.

than did Wagner and Engelhardt³³. These two studies do not offer a good agreement as it is shown in Fig. 5. As a basis of comparison in the Ag-Au system, the compilation done by Hultgren et al²² and based mainly on Oriani's work³⁴ will be used in this study. That compilation reduced to 1200°K is given in Table 3.

TABLE 3. Thermodynamic Properties of Liquid Ag-Au Alloys at 1200°K, according to Hultgren et al²².

X_{Ag}	Ag	Au	G_*^E	H_*^M	S_*^E	TS_*^E
0.1	0.045	0.893	-266	-410	-0.12	-144
0.2	0.102	0.775	-456	-720	-0.22	-264
0.3	0.173	0.654	-582	-930	-0.29	-348
0.4	0.256	0.522	-644	-1040	-0.33	-396
0.5	0.366	0.399	-652	-1060	-0.34	-408
0.6	0.485	0.279	-604	-1000	-0.33	-396
0.7	0.619	0.178	-512	-860	-0.29	-348
0.8	0.756	0.097	-376	-640	-0.22	-264
0.9	0.886	0.038	-206	-350	-0.12	-144

* Values of G_*^E , H_*^M , S_*^E , and TS_*^E are given in cal/gfw.

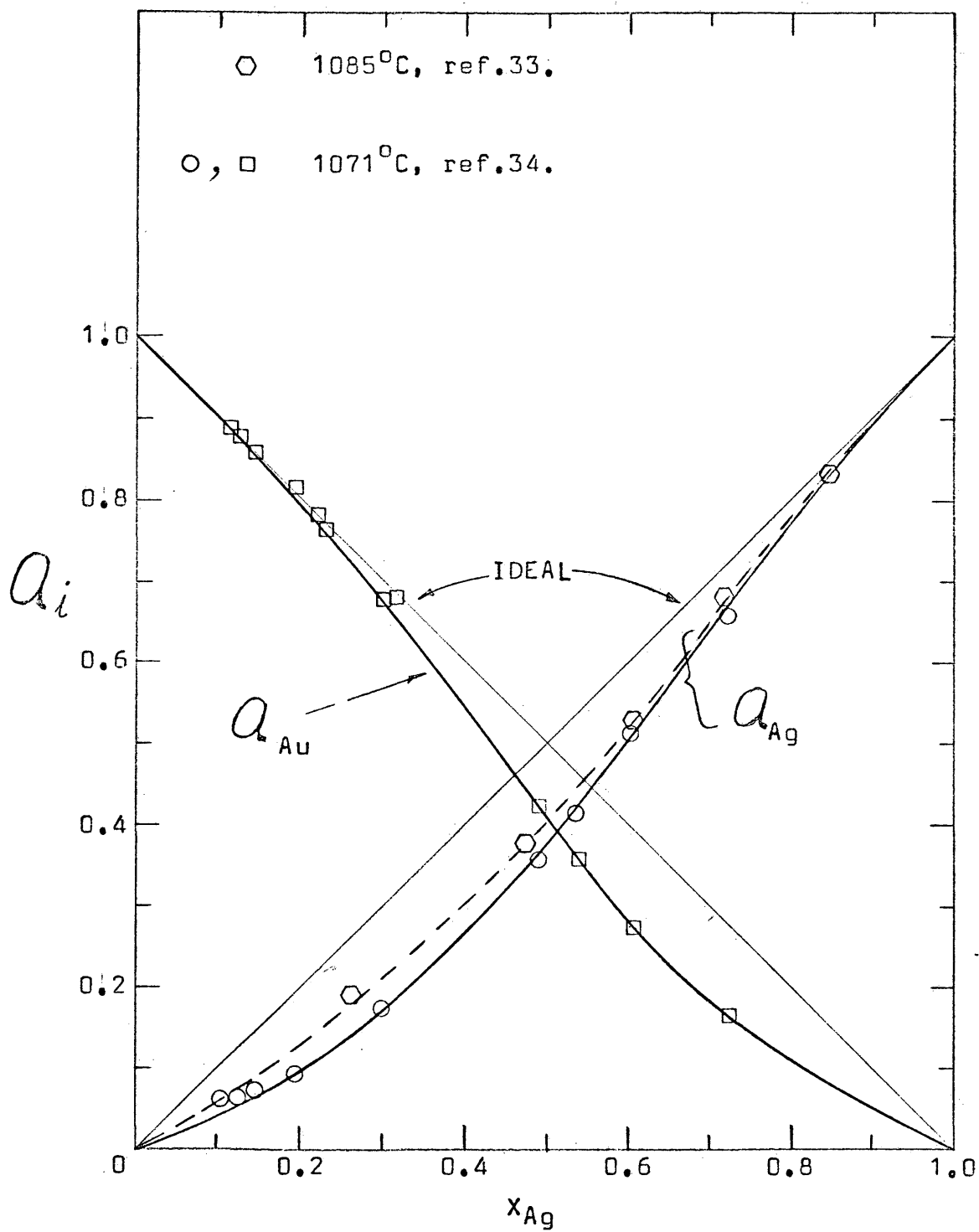


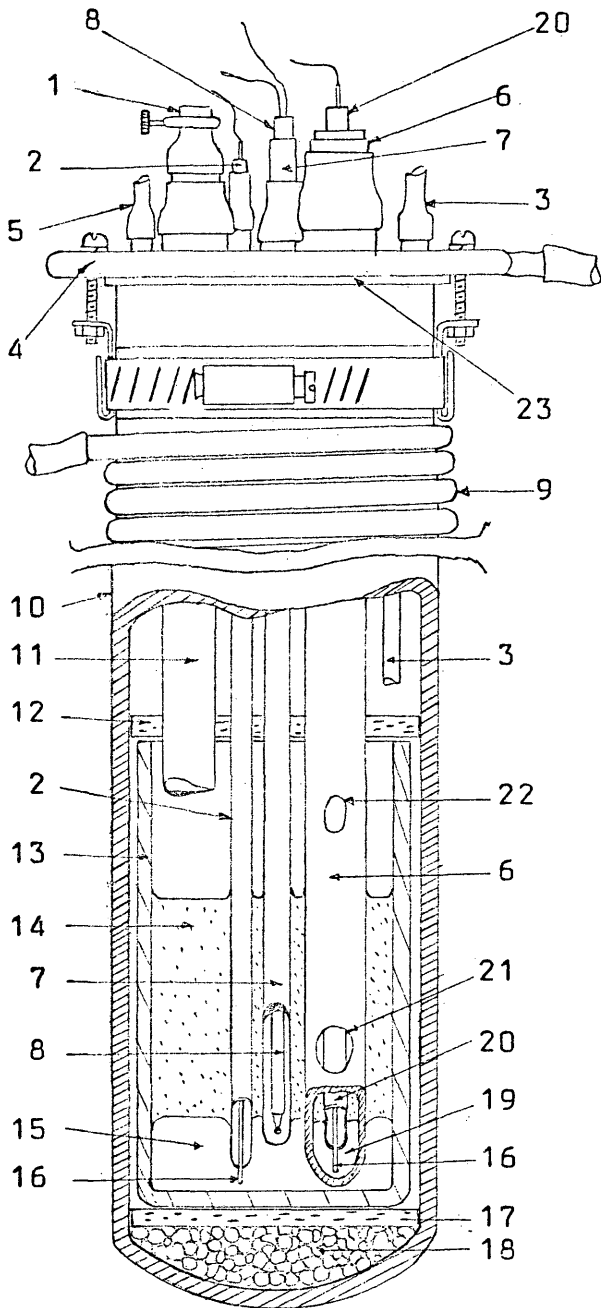
Fig. 5. Activities of silver and of gold in their liquid alloys, relative to the pure liquids.

III. APPARATUS AND EXPERIMENTAL PROCEDURES

The relative chemical potential of lead in homogeneous liquid lead-silver-gold alloys is determined using a concentration cell to cover the temperature range from 775^o - 1030^oC. Having selected a X_{Ag}/X_{Au} ratio, the concentration of lead was varied from $X_{Pb} = 0.1$ to $X_{Pb} = 0.9$, and the e.m.f. of each alloy was recorded as a function of temperature.

A. Description of the Apparatus.

The Galvanic Cell Apparatus: The galvanic cell arrangement is shown pictorially in Fig. 6 and schematically in Fig. 7. The crucible for this cell was made of pure opaque quartz supplied by the Thermal American Fused Quartz Co. The cell dimensions were 1-3/8 inches inside diameter by 4 inches high. The entire cell assembly was contained in a Coors Mullite tube, 2 inches inside diameter. The standard electrode container was made of transparent quartz tubing 10mm inside diameter with two holes blown in one side, the lower for completion of the electrolyte bridge, and the upper for the gas release when the electrolyte entered through the lower hole.



1. Sample and Addition Port
2. Alloy Electrode Lead Wire in Quartz Tube.
3. Argon Outlet
4. Water Cooled Brass Head
5. Argon Inlet
6. Standard Electrode Quartz Tubing
7. Quartz Thermocouple Protection Tube
8. Pt,Pt-Rh Measuring Thermocouple
9. Copper Cooling Coil
10. Mullite Reaction Tube
11. Vycor Addition Tube
12. Alundum Crucible Cover
13. Quartz Crucible
14. $PbO-SiO_2$ Electrolyte
15. Pb-Ag-Au Alloy Electrode
16. Molybdenum Electrode Lead Wires
17. Alundum Crucible Support
18. Porcelain Beads
19. Pb Standard Electrode
20. Standard Electrode Lead Wire in Quartz Tubing
21. Electrolyte Window
22. Gas Vent
23. Silicon Rubber Gasket

FIG. 6 GALVANIC CELL DESIGN

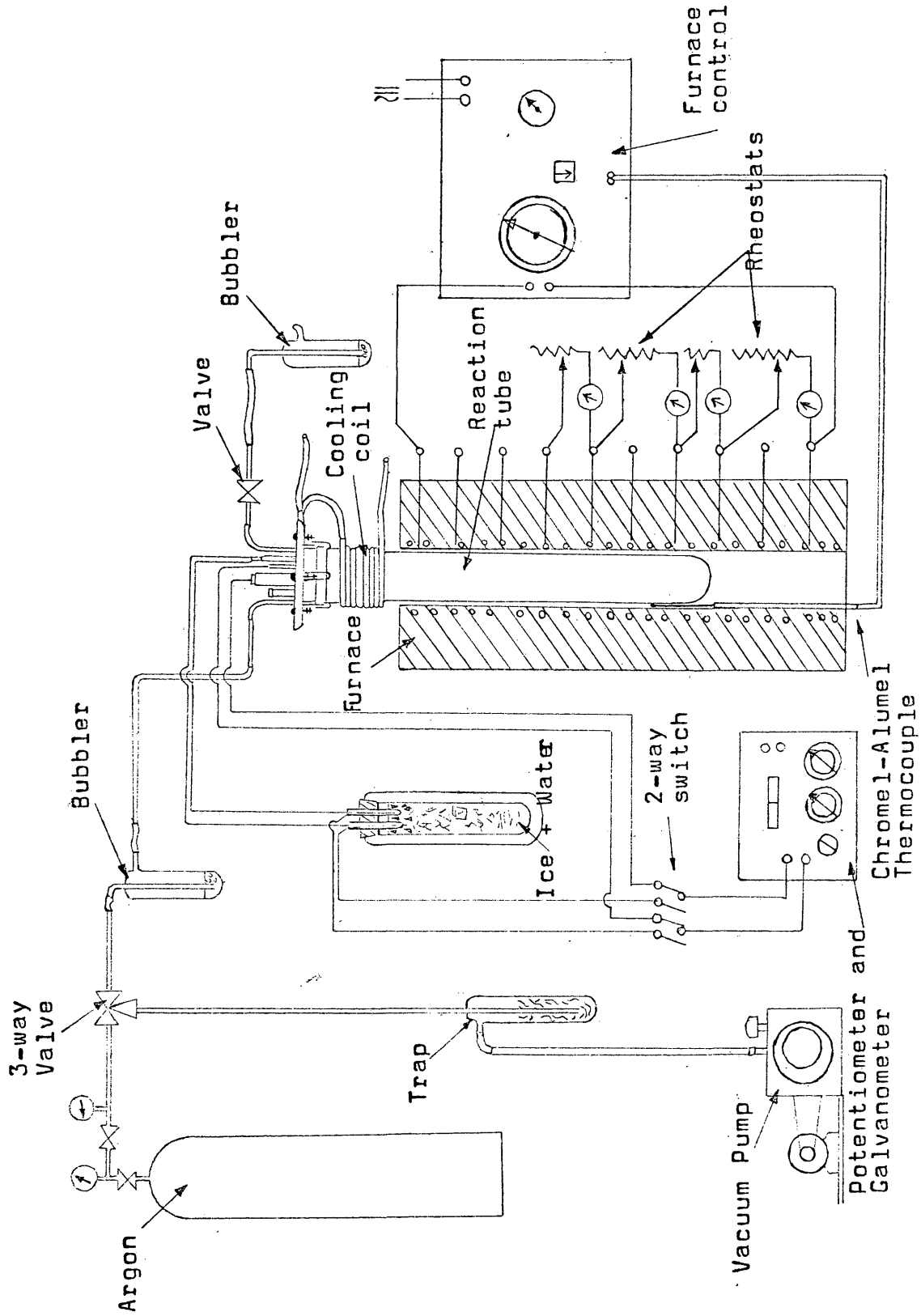


FIG. 7 SCHEMATIC VIEW OF THE EQUIPMENT ARRANGEMENT.

The electrode lead wires were 0.05 inch diameter Molybdenum wire from Fansteel, and protected by 2mm inside diameter quartz tubing, fused to the wire at the lower end. Exact temperatures inside the cell were obtained by means of a calibrated Pt-Pt,10% Rh thermocouple (see Appendix C for calibration of the thermocouple).

High purity Coors Alumina was used for the thermocouple insulators, and a 3mm inside diameter quartz tubing as the protection shield. Addition and sampling tubes were Vycor of 9mm and 6mm inside diameter respectively. A water-cooled brass head with suitable fittings permitted the entry of the standard electrode tube, the thermocouple protection tube, the electrode lead wire protections, the addition tube, and the gas-vacuum connections. A 3/8 inch thick Norton Alumdum-disc with convenient holes for electrodes and tubes was used as the cell cover and as a radiation shield.

The reaction tube was inserted in a vertical Marshall Resistance Furnace. The reaction tube was connected to a three-way valve to permit either application of a vacuum or Argon gas to the cell. Two bubblers containing dibutylphthalate provided a gas seal for the reaction tube. A schematic view of the gas system is also shown in Fig. 7.

B. Experimental Procedure.

1. Materials and Material Preparations. There were two materials to be prepared for each run in the Galvanic Cell: the electrolyte and the alloys. The initial step was to prepare the electrolyte which was liquid lead-oxide saturated in silica. The lead oxide was 99.9% minimum purity, and the silica was of pure chromatographic grade, 50/200 mesh. A mixture of 33 wt-% silica and 67 wt-% PbO was used because this particular composition was in the area of liquid + $\text{SiO}_2(\text{s})$, which would insure a silica-saturated melt at all temperatures considered in this study. Therefore, the silica tubing and crucible apparatus would not be attacked. This mixture of PbO- SiO_2 was heated in a 525 cc silica crucible in a gas-fired furnace at 950°C for 30 minutes. The melt was cast into a steel die and then crushed to -6 mesh. During this study, three different batches of 1500 grams each were prepared at different times. All of the electrolytes exhibited the same pale yellow color with some precipitated silica.

The alloys were prepared from lead, silver, and gold. The lead and silver assayed 99.99+% and were purchased from American Smelting and Refining Co. The gold was also 99.99+% and was donated by Kennecott Copper Corp. for this study. These materials could be added directly to the cell by means of the addition tube. Complete analysis of all materials is given in Appendix D.

2. Galvanic Cell Measurements. After adding about 220 grams of the previously prepared electrolyte to the cell crucible, the parts of the cell were assembled in the manner shown in Fig. 7. The reaction tube was evacuated and a slow flow of Argon started while the furnace was heated slowly. The furnace was allowed to heat slowly (18 hours) to about 950°C when the standard electrode tube containing the pure lead (anode) was lowered quickly into the melt. The alloys were next added through the addition tube to give about 90 grams of alloy. The lead and silver were granular and the gold foil was cut into small pieces for easy addition. The cell was held at 950°C for 18 hours to permit the alloy to become completely homogeneous and to reach equilibrium with the electrolyte. The e.m.f. readings were then taken approximately in the following temperature sequence: 1030-1000-950-900-850-800-775-825-925 $^{\circ}\text{C}$, allowing about 5 hours for the cell to reach equilibrium after each change in temperature. At the end of this period, readings were taken every 15 minutes until a constant value was obtained. After the complete temperature range was studied, a sample was taken at about 950°C . Additional lead was then dropped into the cell through the addition tube, and the cell was again allowed to homogenize for 18 hours before the new series of readings was started.

The cell were operated for three weeks with no sign of deterioration. The electrolyte was very clear at the end of this time.

3. Sampling Technique. Samples were taken of each alloy for atomi-absorption analysis. Sample rods were obtained by lowering a 4mm diameter quartz tube into the liquid alloy through the addition tube. Convenient amounts of alloy were sucked into the tubing with a syringe. The sample tube was quickly removed from the cell and quenched in water to prevent segregation. The analytical technique for the chemical analysis of samples is given in Appendix F.

4. Temperature Measurements. Temperature control was by means of a Foxboro-mechanical controller, with the controlling thermocouple inserted between the furnace tube and the reaction tube. The temperature was kept within $\pm 0.5^{\circ}\text{C}$ in a lenth of 5 inches.

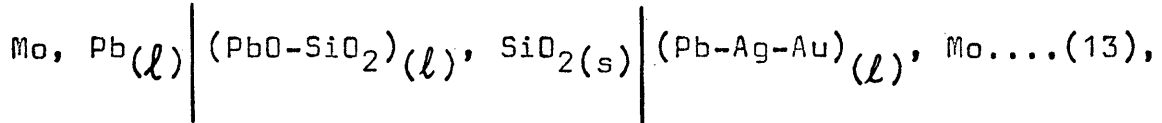
Potential of the cell and of the thermocouple were measured with a Leeds and Northrup Potentiometer Model 8687 by means of the null method. The limits of error in the readings were 0.04% of reading + $3\mu\text{v}$.

IV. REDUCTION OF EXPERIMENTAL DATA

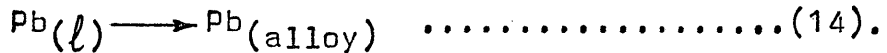
The raw experimental data are converted into the thermodynamic properties by means of the pertinent equations as will be explained later in this section. Also an analysis of the uncertainties of each thermodynamic property is presented to show the experimental limits of accuracy of this study.

A. Thermodynamic Computations.

In a Galvanic Cell of the type:



the overall cell reaction is:



The change in free energy for this reaction is calculated by the expression:

$$\Delta G = \mu_{\text{Pb}(\text{alloy})} - \mu_{\text{Pb}(l)}^{\circ} = - nFE \dots \dots \dots (15)$$

where,

$\mu_{\text{Pb}(\text{alloy})}$: is the chemical potential of lead in the liquid alloy at temperature T.

$\mu_{\text{Pb}(l)}^{\circ}$: is the chemical potential of pure liquid lead at temperature T.

F; is the Faraday constant(23,063 cal/volt-equivalent)

E: is the potential of the cell in volts, and

n: is the number of equivalents of lead oxidized at the anode.

The value of n was not experimentally determined in this study and was taken as 2.0, since previous works^{14,15,4,5} have shown the PbO-SiO₂ melts to be essentially ionic conductors.

Since $\mu_{Pb(\text{alloy})}$ can be expressed in the form:

$$\mu_{Pb(\text{alloy})} = \mu_{Pb(l)}^0 + RT \ln a_{Pb(l)} \dots\dots\dots(16)$$

where,

$a_{Pb(l)}$: is the activity of liquid lead in the liquid alloy, equation (15)

becomes:

$$\mu_{Pb(l)}^0 + RT \ln a_{Pb(l)} - \mu_{Pb(l)}^0 = -nFE$$

$$\therefore a_{Pb(l)} = \exp(-nFE/RT) \dots\dots\dots(17).$$

The activity coefficient of lead is defined by the expression:

$$\gamma_{Pb} = a_{Pb}/X_{Pb} \dots\dots\dots(18).$$

Also, according to equation (5),

$$G_{Pb}^M = RT \ln a_{Pb}, \text{ and by definition,}$$

$$G_{Pb}^E = G_{Pb}^M - G_{Pb(\text{ideal})}^M = -nFE - RT \ln(X_{Pb}) \dots\dots\dots(19).$$

Through a similar analytical procedure, the following relative partial molar properties of lead are obtained:

$$H_{Pb}^M = -nF \left[E - T(\partial E / \partial T) \right]_{P, X_{Pb}} \dots\dots\dots(20)$$

$$S_{Pb}^E = nF(\partial E / \partial T)_{P, X_{Pb}} + R \ln(X_{Pb}) \dots\dots\dots(21)$$

The alpha and beta functions of lead are defined as follows:

$$\alpha_{Pb} \equiv G_{Pb}^E / (1 - X_{Pb})^2 = RT \ln(\gamma_{Pb}) / (1 - X_{Pb})^2 \dots\dots\dots(22)$$

$$\beta_{Pb} \equiv H_{Pb}^M / (1 - X_{Pb})^2 \dots\dots\dots(23)$$

To obtain the Excess Integral Molar Free Energy of Mixing (G^E), and the Integral Molar Heat of Mixing (H^M) for the Pb-Ag-Au system, the following equation first derived by Darken³⁵ is used:

$$Y = (1 - X_2) \left[\int_1^{X_2} \bar{Y}_2 / (1 - X_2)^2 dX_2 \right]_{X_1/X_3} + X_1 \left[\int_0^1 \bar{Y}_2 / (1 - X_2)^2 dX_2 \right]_{X_3=0} + X_3 \left[\int_0^1 \bar{Y}_2 / (1 - X_2)^2 dX_2 \right]_{X_1=0} \dots\dots\dots(24),$$

where,

Y: is the molar value of any extensive property,

\bar{Y}_2 : is the corresponding partial molar quantity for the less noble metal(Pb).

The last two terms in brackets in equation (24) represent the area under the α_{Pb} or β_{Pb} vs. X_{Pb} plots in the Pb-Ag and Pb-Au systems respectively.

The first term in brackets represents the area under the α_{pb} or β_{pb} vs. X_{pb} plots for each pseudo-binary from $X_{pb} = 1$ to some $X_{pb} = X'_{pb}$.

Now, for a ternary system,

$$X_1 + X_2 + X_3 = 1$$

$$\therefore X_1 + X_3 = 1 - X_2 \dots\dots\dots(25)$$

Also, for each pseudo-binary,

$$X_1/X_3 = R = \text{constant}$$

$$X_1 = R \times X_3 \dots\dots\dots(26)$$

Combining equations (25) and (26), we get:

$$\left. \begin{aligned} X_1 &= R(1-X_2)/(1+R) \\ X_3 &= (1-X_2)/(1+R) \end{aligned} \right\} \dots\dots\dots(27)$$

Combining equations (24) and (27)s, we get:

$$Y = (1-X_2) \left\{ \left[\int_1^{X_2} \frac{\bar{Y}_2}{(1-X_2)^2} dX_2 \right]_{X_1/X_3} + R/(1+R) \left[\int_0^1 \frac{\bar{Y}_2}{(1-X_2)^2} dX_2 \right]_{X_3=0} \right. \\ \left. + 1/(1+R) \left[\int_0^1 \frac{\bar{Y}_2}{(1-X_2)^2} dX_2 \right]_{X_1=0} \right\} \dots\dots\dots(28)$$

After the Integral Molar Properties for the ternary Pb-Ag-Au system have been obtained, a plot of G^E vs. Composition in the ternary field is constructed. From this plot, G_{Ag}^E and G_{Au}^E along selected pseudo-binaries are obtained by means of the slope-intercept method according to the following equations:

$$\left. \begin{aligned}
 G_{Ag}^E &= G^E + (1-X_{Ag}) \left[\left(\frac{\partial G^E}{\partial X_{Ag}} \right)_{X_{Pb}/X_{Au}} \right] \\
 G_{Au}^E &= G^E + (1-X_{Au}) \left[\left(\frac{\partial G^E}{\partial X_{Au}} \right)_{X_{Pb}/X_{Ag}} \right]
 \end{aligned} \right\} \dots\dots\dots(29)$$

From the G_{Ag}^E and G_{Au}^E values, the activities of Ag and Au were calculated to plot the isoactivities of these two components according to the following equations:

$$G_i^E = RT \ln(\gamma_i) \dots\dots\dots(30)$$

$$a_i = \gamma_i \times X_i \dots\dots\dots(31)$$

It is well known that the defining equations for the thermodynamic functions have the inconvenience of being too sensitive for the precision the experimental results possess at high mole fractions of the less noble metal; therefore, the thermodynamic properties derived by Gibbs-Duhem integration depend exceedingly on how well these functions are experimentally defined.

In a multicomponent system there are at least three different ways for the experimental data to be taken:

- 1) Many pseudo-binaries examined as completely as possible (many compositions on each of them).
 - 2) Many pseudo-binaries with a modest number of compositions.
 - 3) A few pseudo-binaries done as completely as possible.
- Since this study belongs to the second category, the

following procedure was followed in order to have a better appreciation of how to draw the α and β functions:

a) The raw α and β values of lead were plotted as a function of X_{pb} for each pseudo-binary and the two binaries.

b) The α and β functions were drawn through the experimental points based on the original shapes of the activity curves.

c) Since it is difficult to attach any statistical meaning to values of α and β functions for $X_i > 0.5$, we kept adjusting these functions, specially at high X_{pb} , in order to get:

1) Consistent α and β functions along the pseudo-binaries and the two binaries, and

2) Consistent α and β functions as a function of "y"³⁶ for constant values of X_{pb} , with "y" defined as follows:

$$y = X_{Au} / (X_{Au} + X_{Ag}) \dots\dots\dots(32)$$

d) After this, values of a_{pb} were re-calculated from the final choice of alpha functions and it was found that these smooth values of activity were within the uncertainty of the experimental results.

The smooth values of alpha and beta functions were used into equation (28) to get G^E and H^M inside the ternary field and in the limiting case of $X_{pb} = 0$. Values of TS^E in the ternary field were obtained by means of the equation,

$$TS^E = H^M - G^E \dots\dots\dots(33)$$

B. Estimation of Uncertainties:

According to the "principle of superposition of errors"³⁷, if a quantity Q is a function of several independent measured quantities X, Y, Z, the error in Q due to errors $\delta X'$, $\delta Y'$, $\delta Z'$, is given by the equation:

$$\delta Q \approx \frac{\partial Q}{\partial X} \cdot \delta X' + \frac{\partial Q}{\partial Y} \cdot \delta Y' + \frac{\partial Q}{\partial Z} \cdot \delta Z' + \dots \dots(34)$$

The total "most provable" value of δQ is given by:

$$\delta Q = \sqrt{(\frac{\partial Q}{\partial X} \cdot \delta X')^2 + (\frac{\partial Q}{\partial Y} \cdot \delta Y')^2 + (\frac{\partial Q}{\partial Z} \cdot \delta Z')^2 + \dots} \dots(35)$$

where,

$\delta X, \delta Y, \delta Z$: maximum absolute values of the errors $\delta X', \delta Y',$ and $\delta Z'$ respectively.

1. Uncertainty in the Temperature Readings. The individual uncertainties in temperature readings are:

a) Uncertainty in the calibration of the thermocouple equal to $\pm 0.3^\circ\text{C}$ (see Appendix C).

b) Uncertainty due to drifts during the run, determined experimentally to be approximately $\pm 0.5^\circ\text{C}$.

c) Uncertainty due to thermal gradient at the interface equal to $\pm 0.5^\circ\text{C}$ (see Appendix E).

The total uncertainty in temperature will be:

$$\delta T = \pm 0.8^\circ\text{C}.$$

2. Uncertainty in the e.m.f. and dE/dT . The total uncertainty in E , determined by means of a least square analysis was:

$$\delta E < 0.03 \text{mv}$$

The total uncertainty in dE/dT was also determined by means of the least square analysis to be:

$$\delta (dE/dT) = \pm 0.005 \text{mv}$$

3. Uncertainty in the Chemical Analysis. The individual uncertainties in the X_{Pb} are:

a) Uncertainty in the chemical analysis performed on three known compositions. The maximum deviation in the knowns was:

$$\delta' X_{Pb} = \pm 0.0015$$

b) Uncertainty in the chemical analysis performed on the alloys studied. The maximum deviation in the chemical analysis of the alloys was:

$$\delta'' X_{Pb} = \pm 0.008$$

The total uncertainty in the mole fraction of lead will be:

$$\delta X_{Pb} = \left[(\delta' X_{Pb})^2 + (\delta'' X_{Pb})^2 \right]^{1/2} = \pm 0.008 \text{ (see Appendix F)}$$

4. Uncertainty in the Activity of Lead. By combining equations (17) and (35), we get:

$$\delta a_{Pb} = \left\{ \left[(E \cdot \delta T/T)^2 - \delta E^2 \right] \left[nF/RT \cdot \exp(-nFE/RT) \right]^2 \right\}^{1/2} \dots\dots\dots (37)$$

The total uncertainty will be:

$$\delta a_{Pb} = \pm 0.0004, \text{ at } X_{Pb} = 0.05$$

5. Uncertainties in H_{Pb}^M , G_{Pb}^E , and S_{Pb}^E . By combining

equations (19), (20), and (21) with equation (35), we get:

$$\delta H_{Pb}^M = (nF) \left[\delta E^2 + (\delta T \cdot dE/dT)^2 + T^2 \cdot \delta(dE/dT)^2 \right]^{1/2} \dots \dots \dots (38)$$

$$\delta G_{Pb}^E = \left\{ (nF \cdot \delta E)^2 + R^2 \left[(\ln X_{Pb} \cdot \delta T)^2 + (T \cdot \delta X_{Pb}^2 / X_{Pb})^2 \right] \right\}^{1/2} \dots (39)$$

$$\delta S_{Pb}^E = \left[(nF)^2 \cdot (dE/dT)^2 + R^2 \delta X_{Pb}^4 \cdot X_{Pb}^{-2} \right]^{1/2} \dots \dots \dots (40)$$

The total uncertainties will be:

$$\delta H_{Pb}^M = \pm 150 \text{ cal. at } X_{Pb} = 0.5$$

$$\delta G_{Pb}^E = \pm 6 \text{ cal. at } X_{Pb} = 0.05$$

$$\delta S_{Pb}^E = \pm 0.4 \text{ cal.}$$

The uncertainties in the corresponding thermodynamic properties of silver and gold are estimated to be three times as large as for lead, due to the existing uncertainty in the ternary Gibbs-Duhem integration.

C. Use of the Computer.

First, by means of the computer the best linear mathematical fit through the experimental points for each mole fraction of lead in each of the five pseudo-binaries was accomplished by the method of least square. From the e.m.f. vs. T equations obtained, raw values of G_{Pb}^E , H_{Pb}^M , α_{Pb} , and β_{Pb} were calculated.

Secondly, the computer was of real assistance in obtaining the best alpha and beta function drawings by means of consecutive trials as explained in the last four paragraphs of the preceding section A.

V. RESULTS

A. E.m.f. Measurements of the Lead-Silver-Gold System.

The experimental data in Appendix G reduced to e.m.f. vs. T equations are presented in Table 4 for each pseudo-binary considered in this study. Also a graphical representation is given in Figs. 8A through 8E.

B. Calculation of the Thermodynamic Properties.

1) Raw values for G_{Pb}^E , H_{Pb}^M , α_{Pb} , and β_{Pb} were calculated through the use of equations (19), (20), (22), and (23). Then the α and β functions were drawn trial after trial to get consistent α and β functions along the pseudo-binaries and as a function of "y". The criterion for stopping the drawing of these α and β functions was the result obtained by equation (28) for G^E and H^M in the limiting case of $X_{Pb} = 0$. At this point, reasonable G^E and H^M vs. X_{Ag} plots in the Ag-Au system were obtained.

In Table 5 are given smooth values of the α functions used in this study and in Table 6 the corresponding smooth values of the β functions.

TABLE 4. Experimental Data for Liquid Pb-Ag-Au Alloys.

X_{Pb}	E, mv^{**}
	$R = X_{Ag}/X_{Au} = 5.627$
0.094	$-33.85 + 151.57 \times 10^{-3} T^*$
0.198	$-35.41 + 106.77 \times 10^{-3} T$
0.297	$-27.67 + 79.75 \times 10^{-3} T$
0.395	$-19.46 + 58.79 \times 10^{-3} T$
0.501	$-11.04 + 40.91 \times 10^{-3} T$
0.604	$-6.56 + 29.07 \times 10^{-3} T$
0.700	$-0.70 + 16.79 \times 10^{-3} T$
0.799	$-1.16 + 11.20 \times 10^{-3} T$
0.915	$0.81 + 3.69 \times 10^{-3} T$
	$R = X_{Ag}/X_{Au} = 2.303$
0.100	$-10.86 + 126.94 \times 10^{-3} T$
0.300	$-21.03 + 71.03 \times 10^{-3} T$
0.397	$-16.21 + 55.52 \times 10^{-3} T$
0.510	$-10.10 + 40.52 \times 10^{-3} T$
0.613	$-7.28 + 29.67 \times 10^{-3} T$
0.700	$-4.87 + 21.86 \times 10^{-3} T$
0.803	$-4.32 + 15.29 \times 10^{-3} T$
0.908	$-3.55 + 8.83 \times 10^{-3} T$

* Temperature in °C.

** Within 0.5% of data.

TABLE 4. Experimental Data for(continued)

$$R = X_{Ag}/X_{Au} = 1.000$$

X_{Pb}	E, mv^{**}
0.100	$-61.46 + 189.69 \times 10^{-3} T^*$
0.302	$- 5.88 + 71.05 \times 10^{-3} T$
0.399	$- 6.81 + 56.30 \times 10^{-3} T$
0.499	$- 6.07 + 39.96 \times 10^{-3} T$
0.600	$0.09 + 26.02 \times 10^{-3} T$
0.701	$2.87 + 15.87 \times 10^{-3} T$
0.797	$2.82 + 9.18 \times 10^{-3} T$
0.901	$1.69 + 4.07 \times 10^{-3} T$

$$R = X_{Ag}/X_{Au} = 0.427$$

0.100	$17.35 + 136.99 \times 10^{-3} T$
0.350	$0.47 + 66.58 \times 10^{-3} T$
0.402	$0.88 + 55.94 \times 10^{-3} T$
0.501	$1.80 + 39.22 \times 10^{-3} T$
0.601	$1.90 + 27.49 \times 10^{-3} T$
0.700	$2.97 + 16.60 \times 10^{-3} T$
0.798	$1.97 + 10.31 \times 10^{-3} T$

* Temperature in $^{\circ}C$.

** Within 0.5% of data.

TABLE 4. Experimental Data for(continued)

$$R = X_{Ag}/X_{Au} = 0.1765$$

<u>X_{Pb}</u>	<u>E, mv**</u>
0.100	35.26 + 138.34 × 10 ⁻³ T*
0.200	25.48 + 97.34 × 10 ⁻³ T
0.302	23.07 + 66.67 × 10 ⁻³ T
0.401	-5.12 + 71.83 × 10 ⁻³ T
0.500	4.50 + 41.93 × 10 ⁻³ T
0.600	4.77 + 27.41 × 10 ⁻³ T
0.705	2.87 + 18.34 × 10 ⁻³ T
0.802	0.48 + 12.22 × 10 ⁻³ T
0.899	0.31 + 5.77 × 10 ⁻³ T

* Temperature in °C.

** Within 0.5% of data.

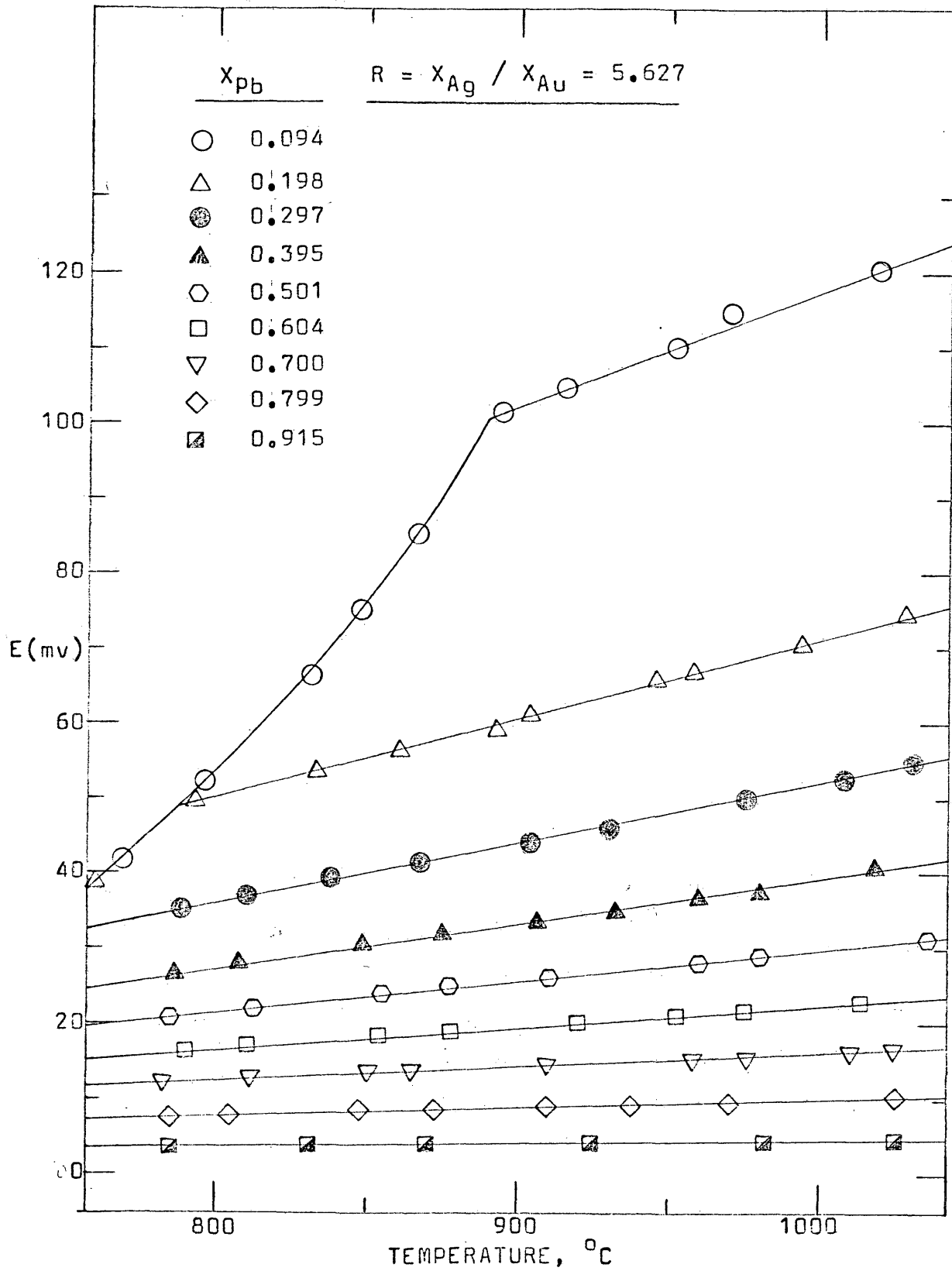


FIG. 8A - EXPERIMENTAL DATA.

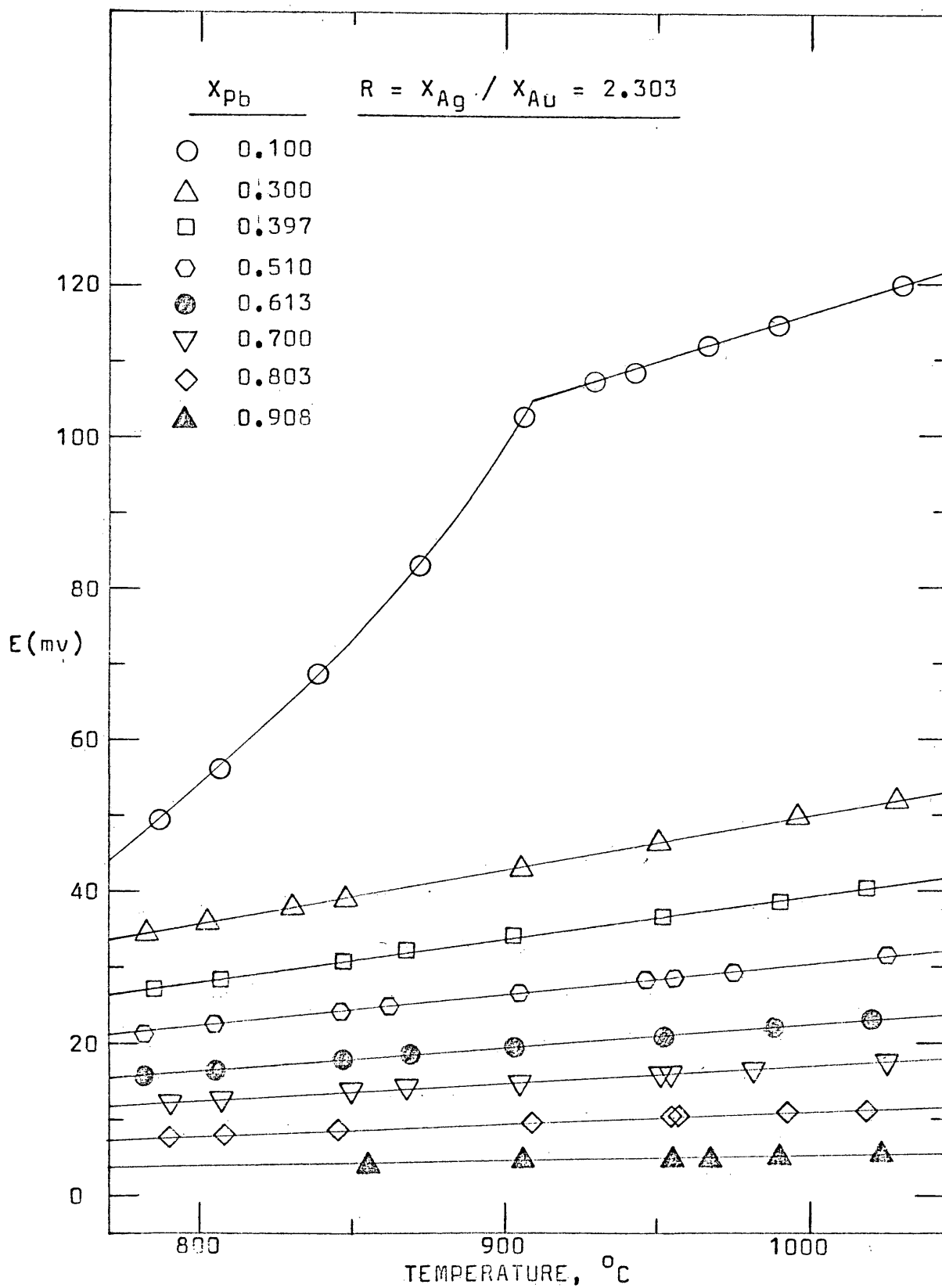


FIG. 88- EXPERIMENTAL DATA.

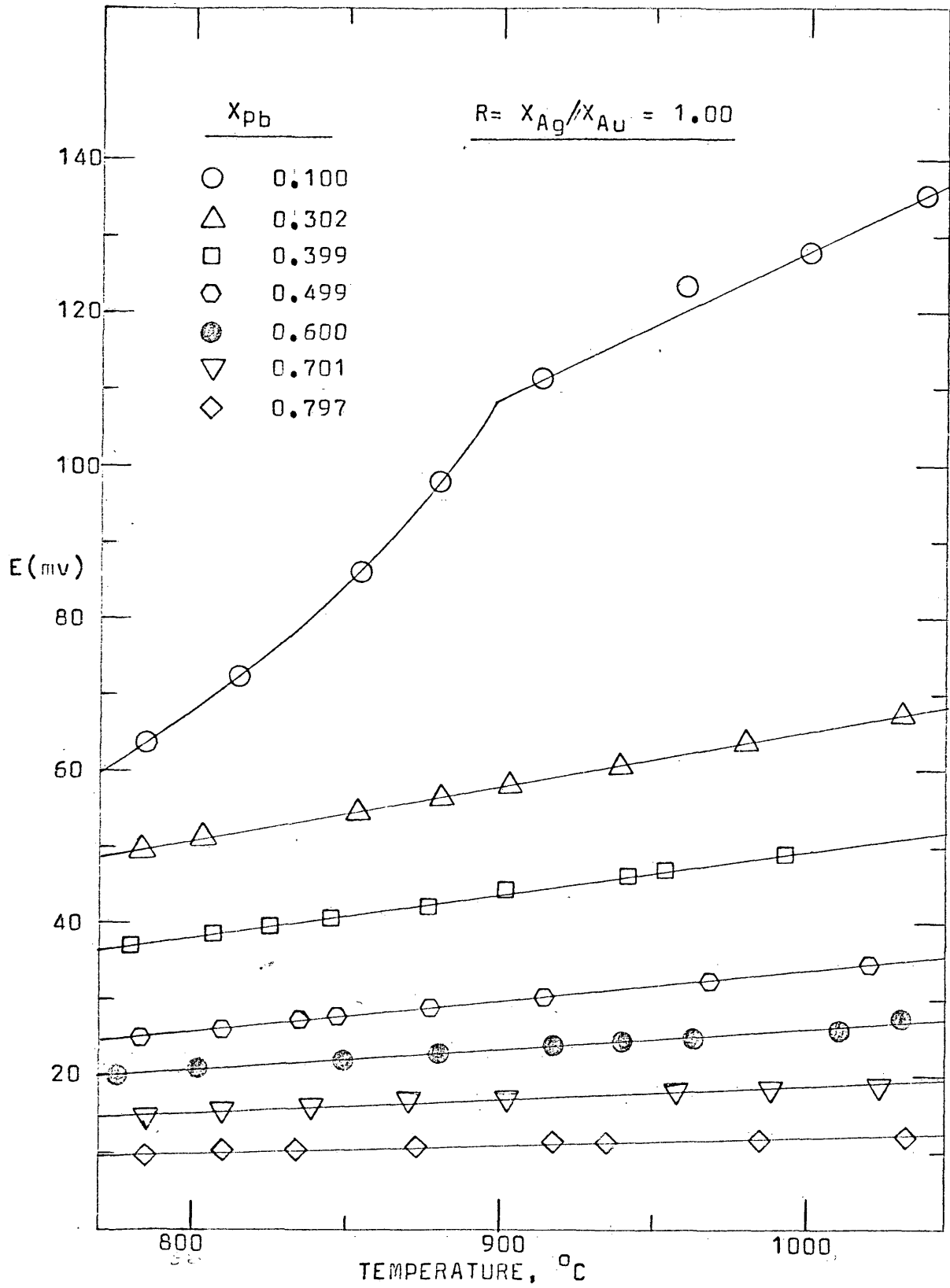


FIG. 8C - EXPERIMENTAL DATA.

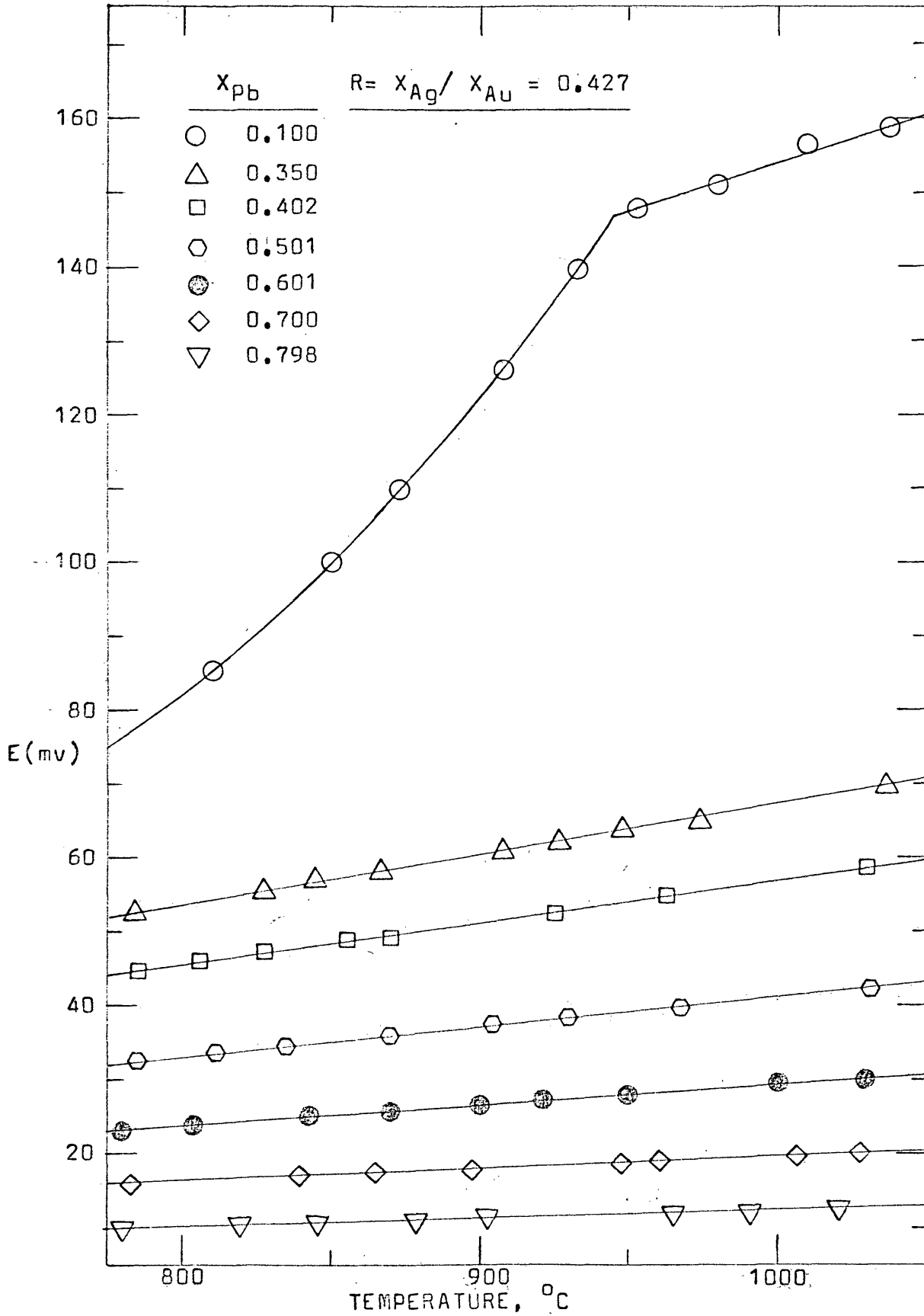


FIG. 8D - EXPERIMENTAL DATA.

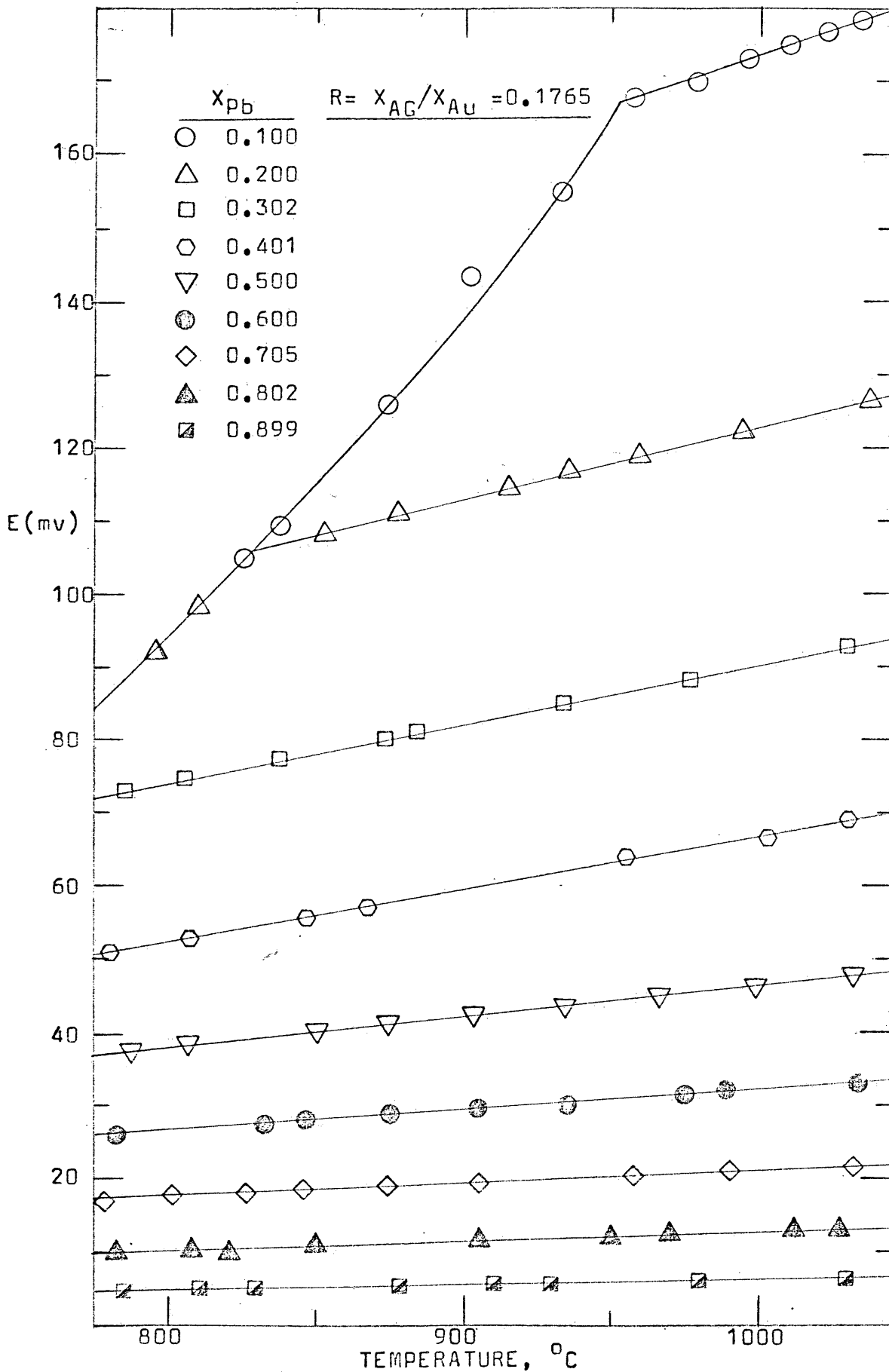


FIG. 8E - EXPERIMENTAL DATA.

TABLE 5. Smooth Values of the Alpha Functions at 1200°K.
(cal/gfw)

X_{Pb} \ R^*	5.627	2.303	1.000	0.427	0.1765
0.0	950	550	120	-1700	-2780
0.1	1150	800	122	-1440	-2565
0.2	1350	1030	139	-1190	-2345
0.3	1530	1240	187	- 945	-2105
0.4	1675	1400	353	- 710	-1820
0.5	1775	1500	905	- 490	-1430
0.6	1825	1525	740	- 290	-1080
0.7	1800	1460	512	- 165	- 920
0.8	1650	1300	423	- 145	- 905
0.9	1500	1090	378	- 235	-1000
1.0	1330	850	348	- 420	-1200

* $R = X_{Ag} / X_{Au}$

TABLE 6. Smooth Values of the Beta Functions at 1200°K.
(cal/gfw)

X_{PB} \ R^*	5.627	2.303	1.000	0.427	0.1765
0.0	3900	4400	4050	2550	640
0.1	4000	4300	3900	2500	740
0.2	4100	4200	3750	2450	840
0.3	4200	4110	3600	2400	980
0.4	4300	4030	3400	2350	1100
0.5	4350	3930	3160	2275	1210
0.6	4350	3830	2960	2180	1340
0.7	4400	3750	2730	2000	1460
0.8	4500	3650	2500	1730	1590
0.9	4600	3550	2200	1350	1710
1.0	4700	3460	1900	900	1840

* $R = X_{Ag} / X_{Au}$

2) Using the final choice of alpha functions, the activities of lead were obtained for each pseudo-binary according to equations (22) and (31) for even mole fractions of lead. Then by interpolation, isoactivities for lead were obtained and are given in Fig. 9a. The a_{Pb} vs. X_{Pb} plots for each pseudo-binary and the two binaries are given in Fig. 9b.

3) The values of G^E and H^M calculated by equation (28) were subject to interpolation to get equal values of G^E and H^M on each pseudo-binary and binary systems. The results are shown in Fig. 10 and Fig. 11 respectively.

4) Five cross sections were made on the contour lines of G^E in the ternary field from the Ag corner to the Pb-Au base at constant X_{Pb}/X_{Au} ratios, and from the Au corner to the Pb-Ag base at constant X_{Pb}/X_{Ag} ratios. By means of the slope-intercept method, G_{Ag}^E and G_{Au}^E were obtained and from these the activities of Ag and Au. The final results are shown in Fig. 12 and Fig. 13 respectively.

5) Finally, using the values of G^E and H^M calculated by equation (28) for each pseudo-binary, the corresponding values of TS^E were calculated by equation (33). The final results are presented in Fig. 14.

6) The α_{Pb} vs. X_{Pb} for the five pseudo-binaries and the two binaries are shown in Fig. 15. Also, α_{Pb} vs. "y" are presented in Fig. 16.

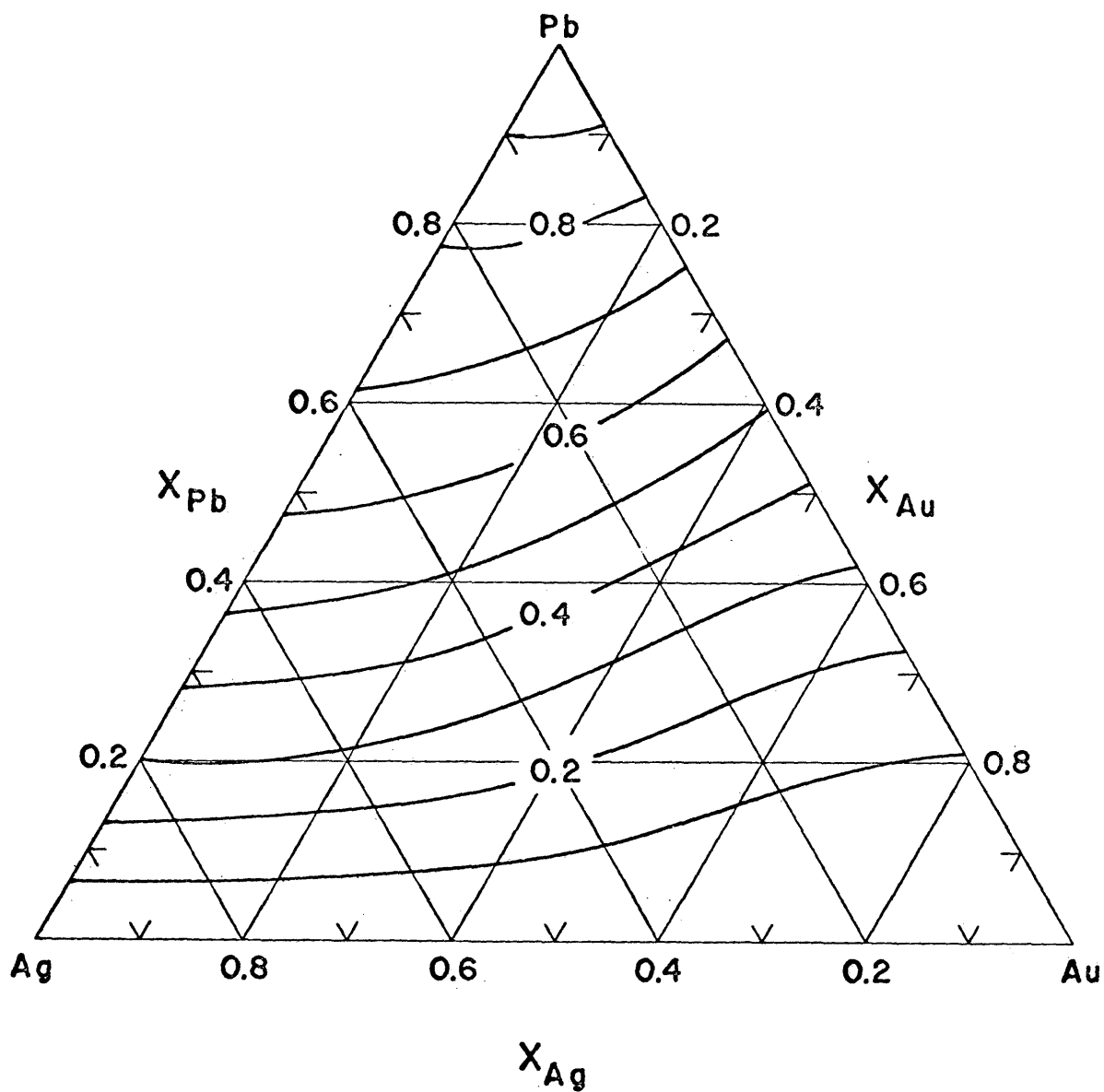


FIG. 9a. ISOACTIVITY LINES FOR LEAD IN THE LIQUID Pb-Ag-Au SYSTEM AT 1200° K.

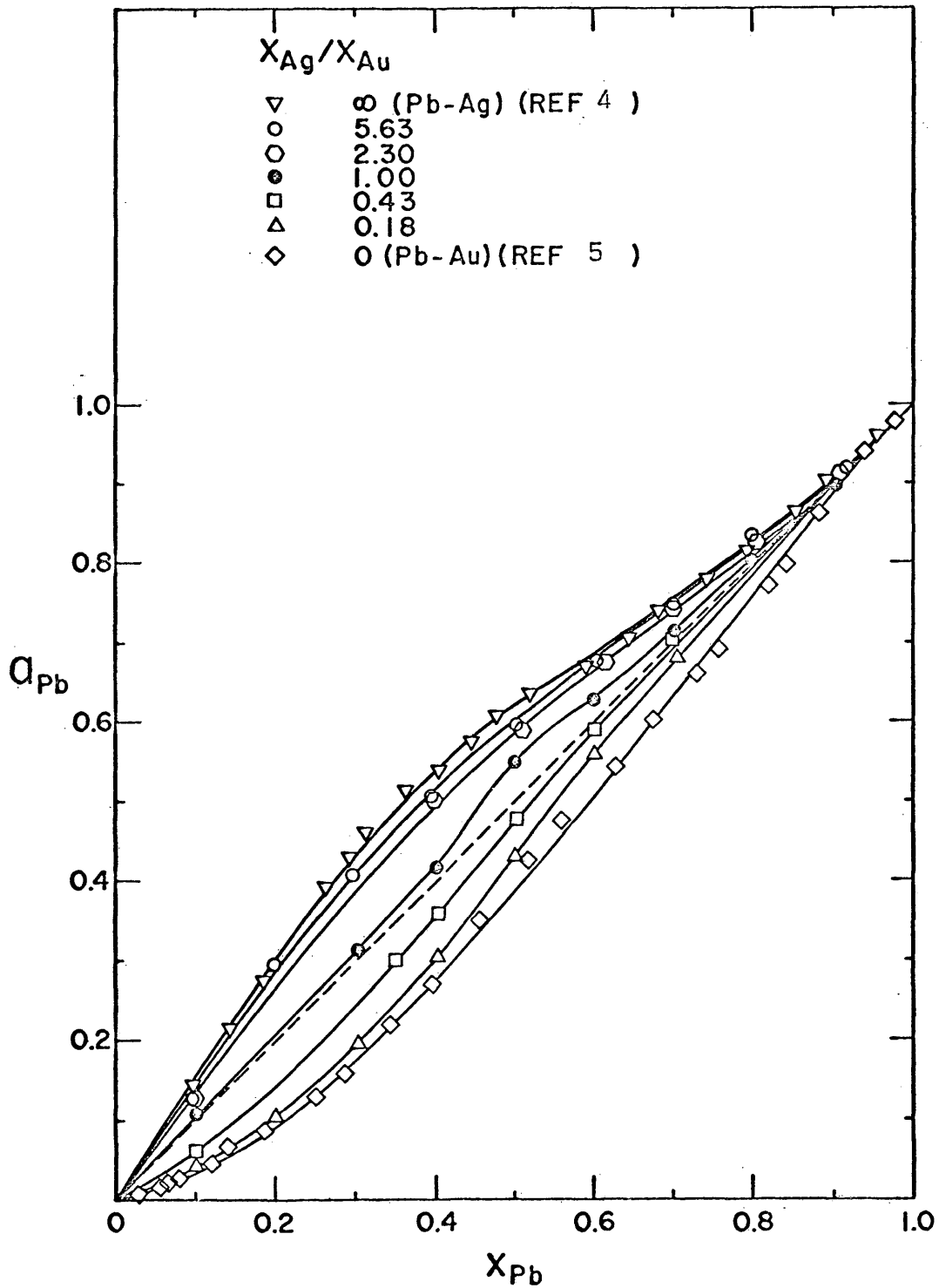


FIG. 9b. ACTIVITY OF LEAD IN THE LIQUID Pb-Ag-Au SYSTEM AT 1200° K.

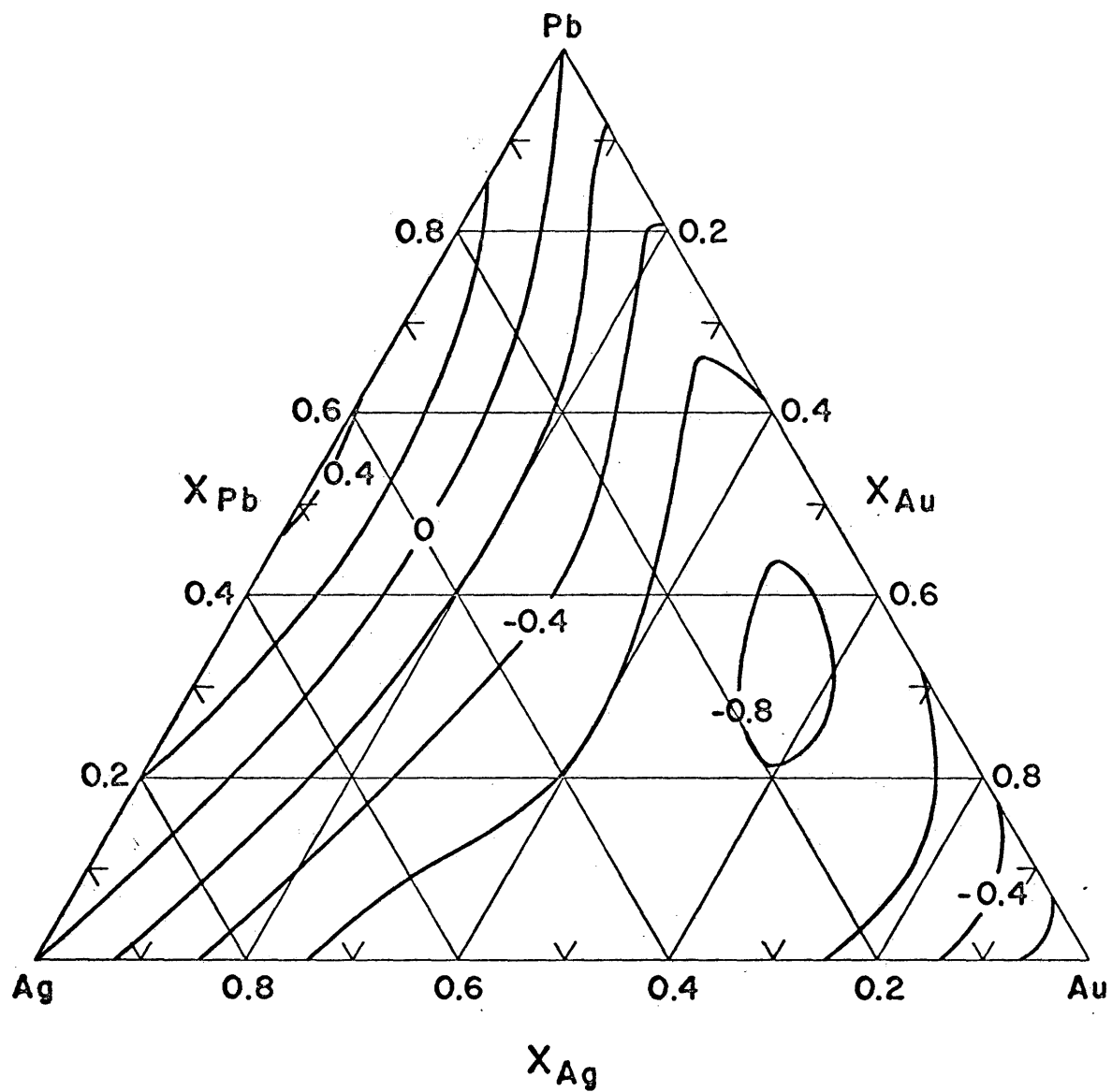


FIG. 10 G^E (IN KCAL PER gfw) OF LIQUID Pb-Ag-Au ALLOYS AT 1200° K.

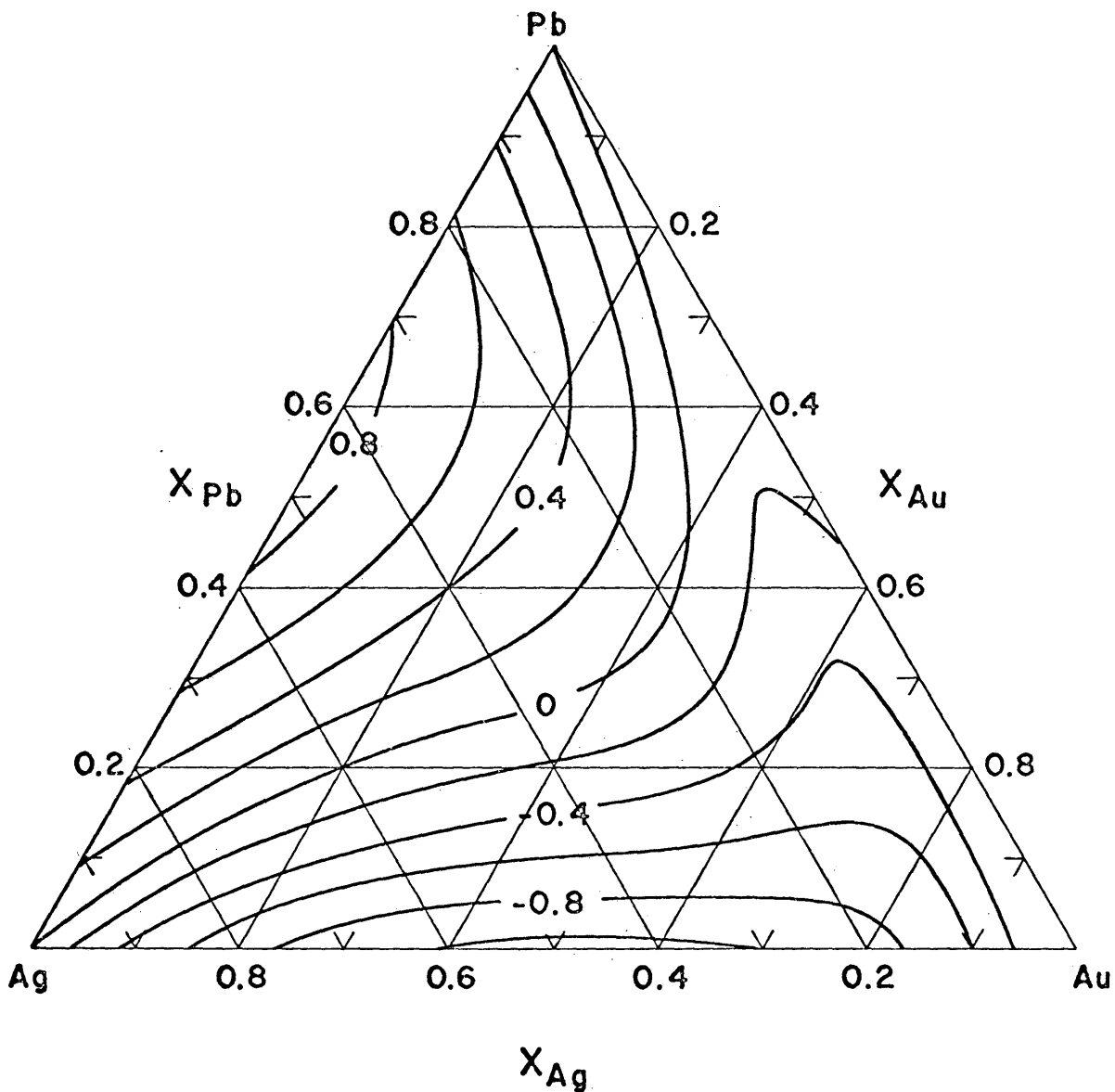


FIG.11. H^M (IN KCAL PER gfw) OF LIQUID Pb-Ag-Au ALLOYS AT 1200° K.

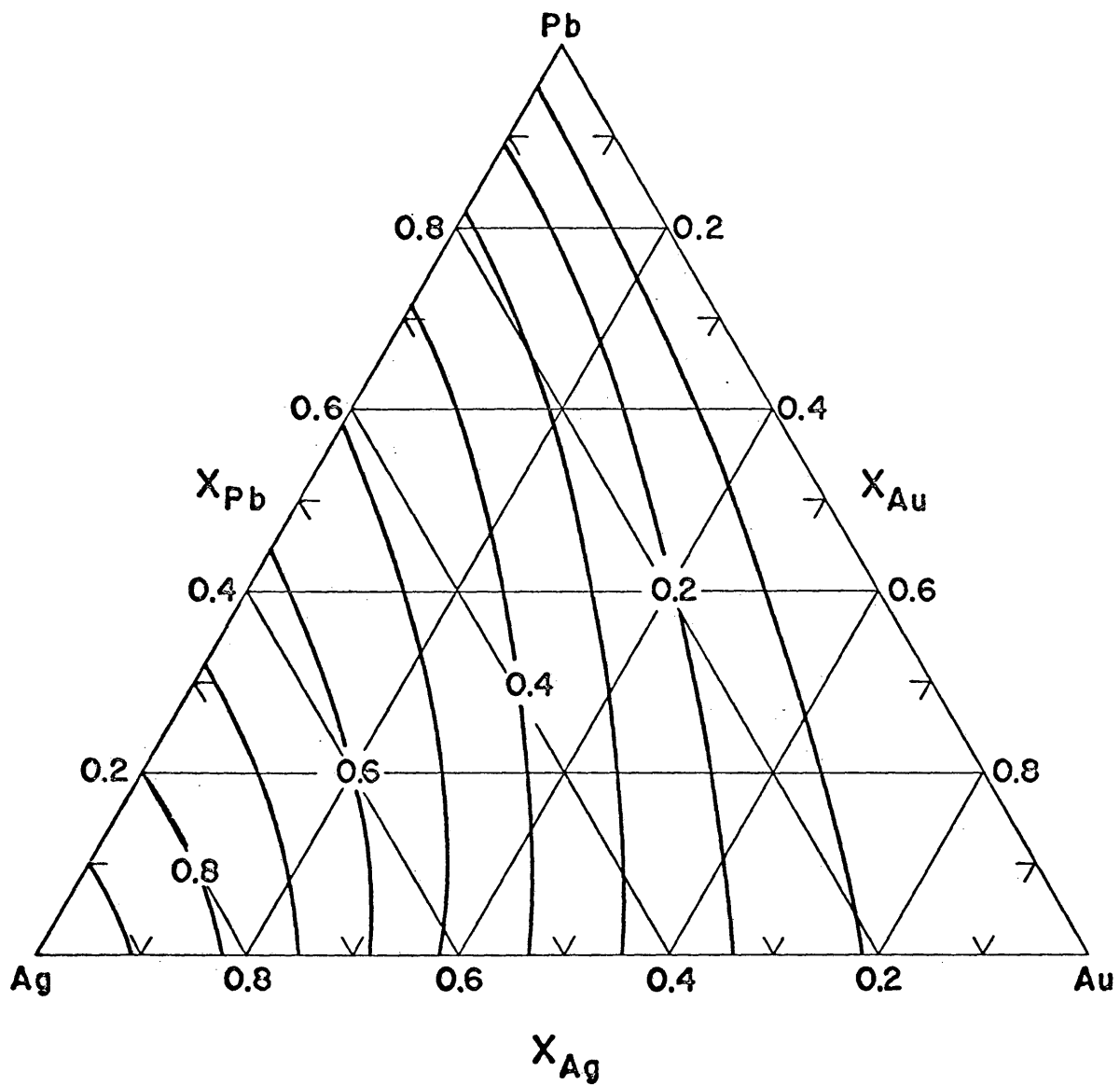


FIG.12. ISOACTIVITY LINES FOR SILVER IN THE LIQUID Pb-Ag-Au SYSTEM AT 1200° K.

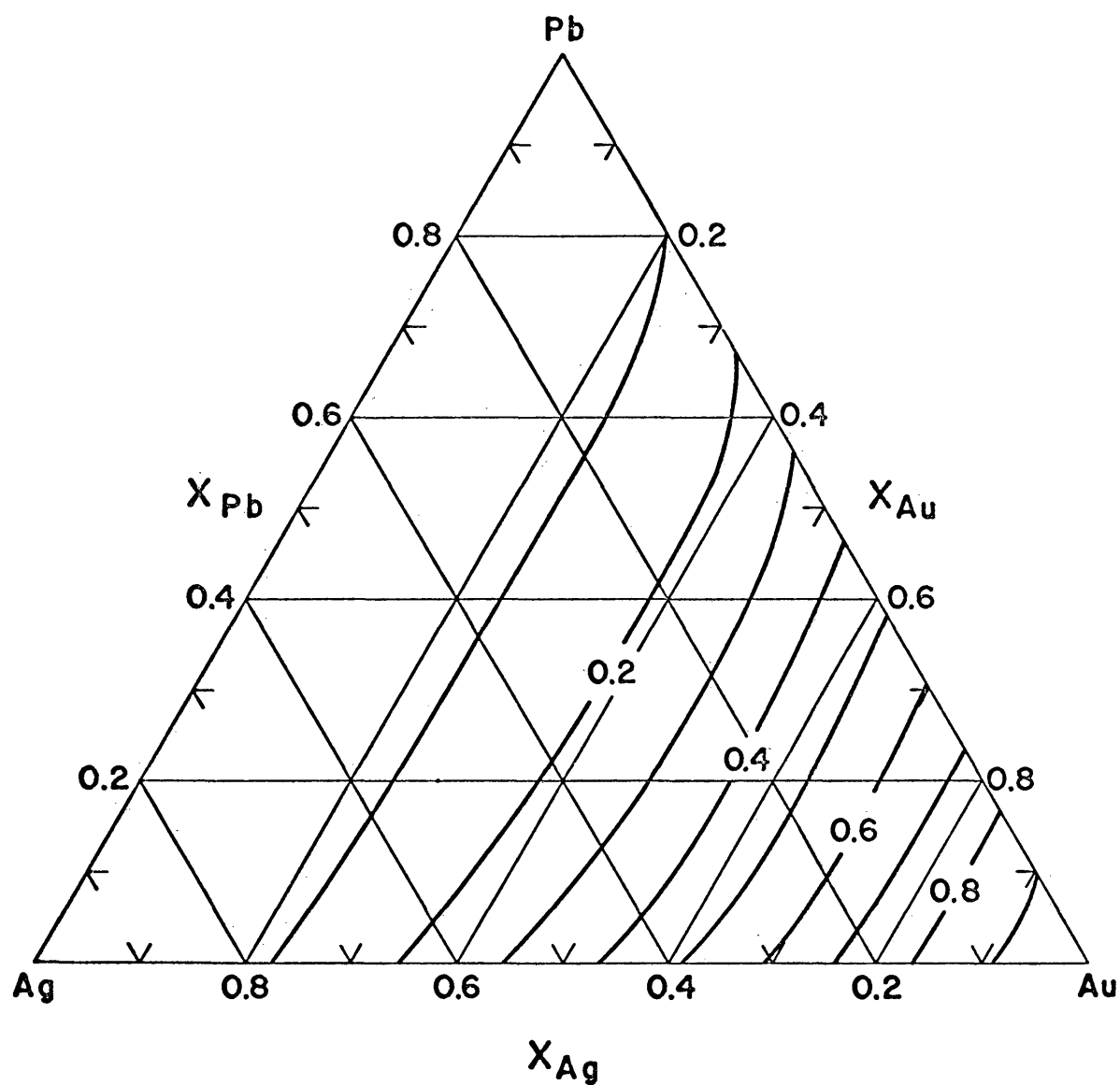


FIG.13. ISOACTIVITY LINES FOR GOLD IN THE LIQUID Pb-Ag-Au SYSTEM AT 1200° K.

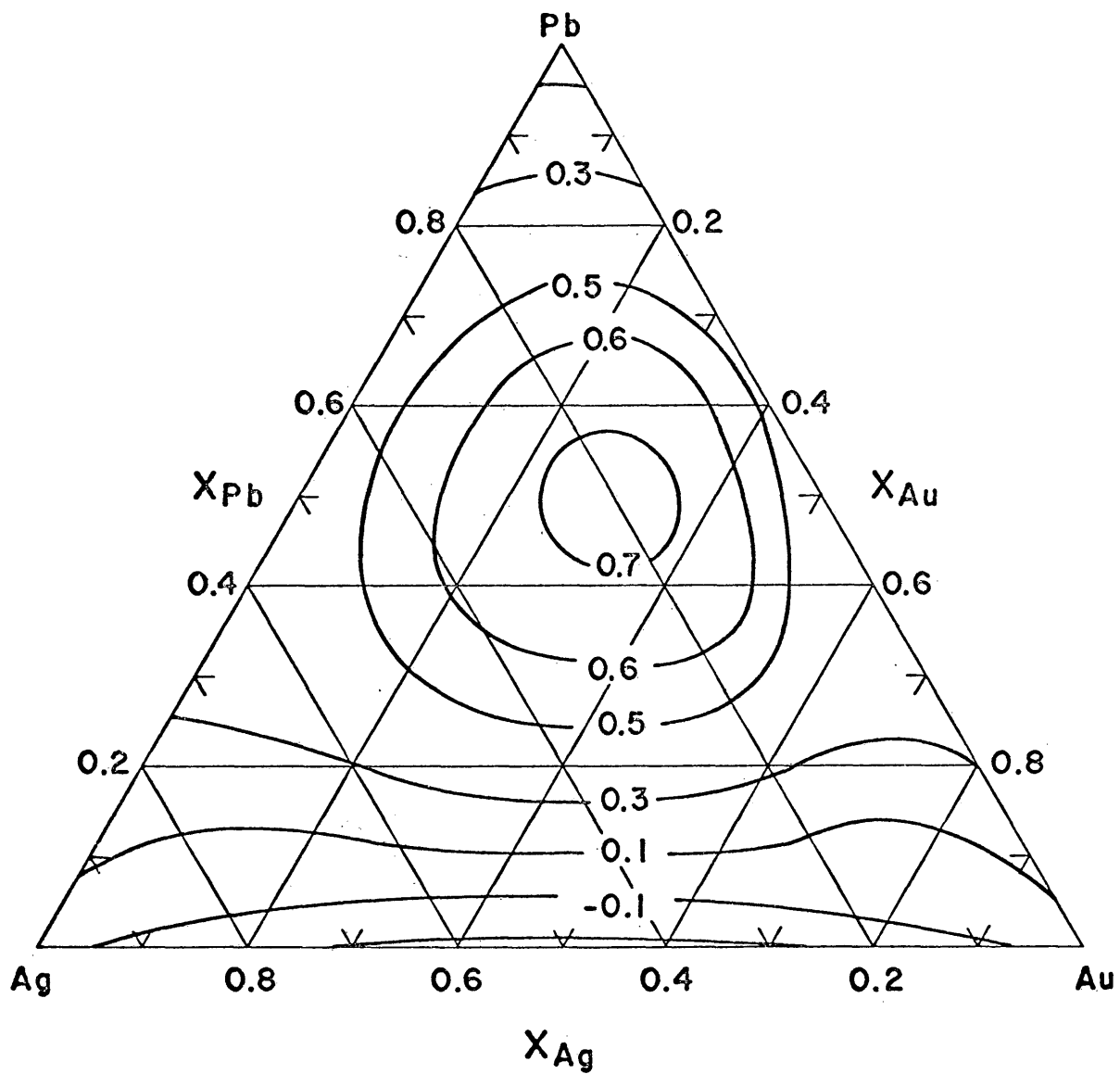


FIG.14. TS^E (IN KCAL PER gfw) OF LIQUID Pb-Ag-Au ALLOYS AT 1200° K.

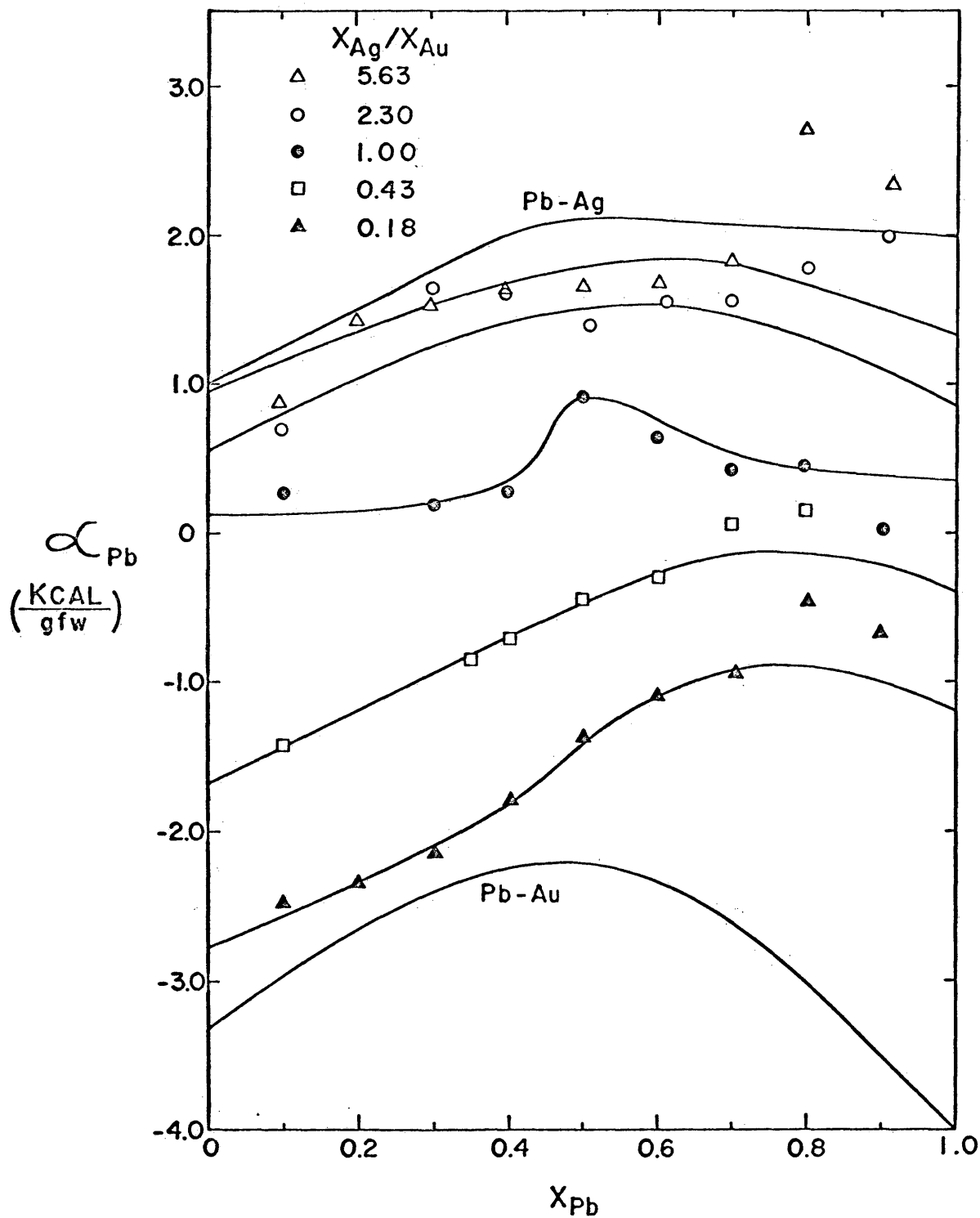


FIG. 15. ALPHA FUNCTION OF LEAD AT 1200° K IN THE LIQUID Pb-Ag-Au SYSTEM.

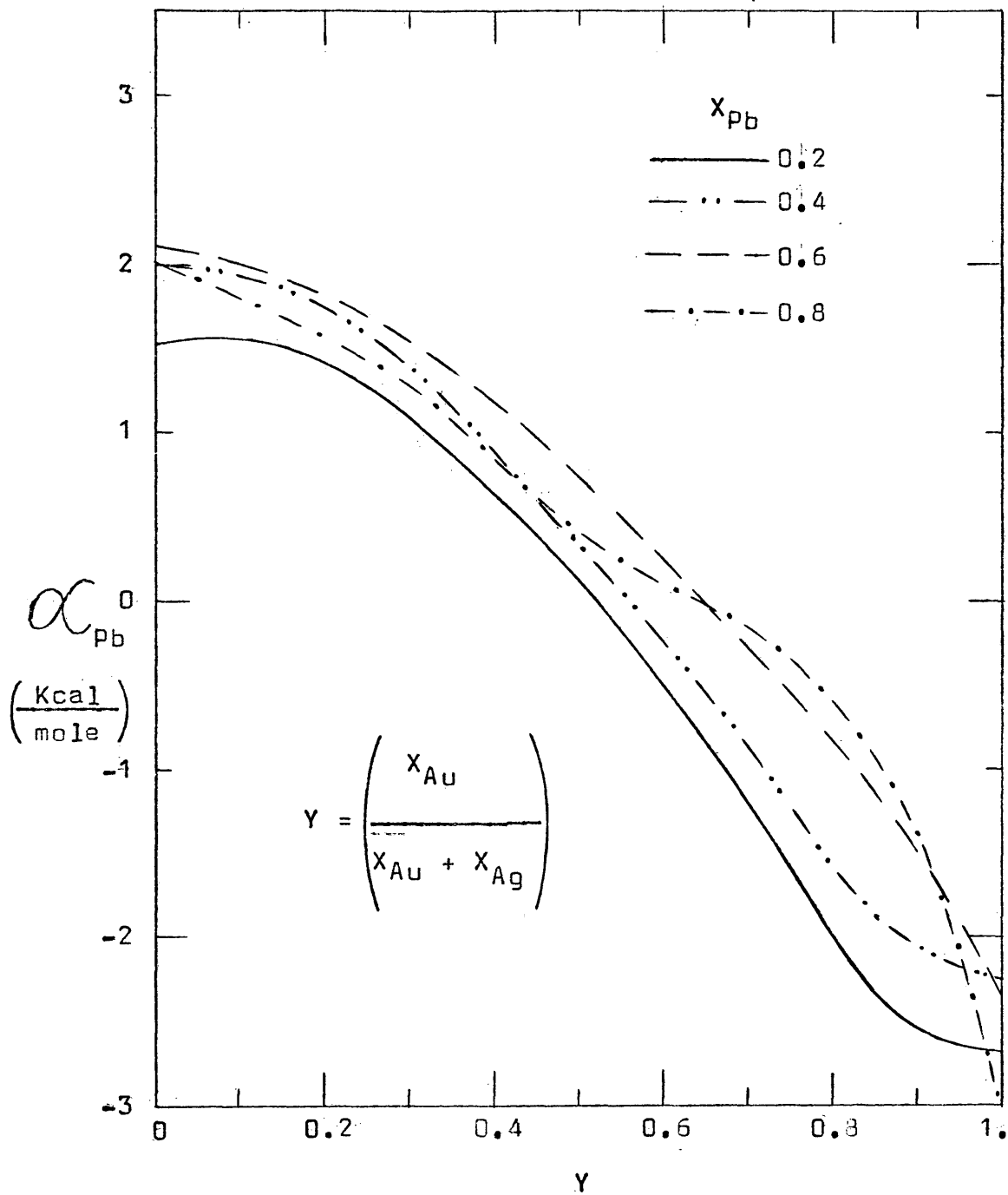


FIG. 16- ALPHA FUNCTIONS OF LEAD IN LIQUID Pb-Ag-Au ALLOYS AT CONSTANT MOLE FRACTIONS OF LEAD AT 1200°K.

VI. DISCUSSIONA. Estimation of the Thermodynamic Properties of the Silver-Gold System.

By means of equation (28), G^E and H^M values were calculated in the limiting case of $X_{PB} = 0$ for the same pseudo-binaries selected to get the thermodynamic properties inside the ternary field. These pseudo-binaries are shown as dashed lines in Fig. 17. Also, the pseudo-binaries to calculate the isoactivities of Ag and Au are indicated on the proper base of the compositional triangle.

Using the equivalent equation to (29), G_{Ag}^E was obtained by the slope-intercept method and from these values the corresponding activities. The alpha function of silver was also calculated to obtain the activities of Au by integration. The comparison of the calculated values for the thermodynamic properties on the Ag-Au base with the compilation done by Hultgren et al²² is presented in Figs. 18 and 19. The agreement is good for a very indirect procedure of calculation and despite the uncertainty of the method of integration itself.

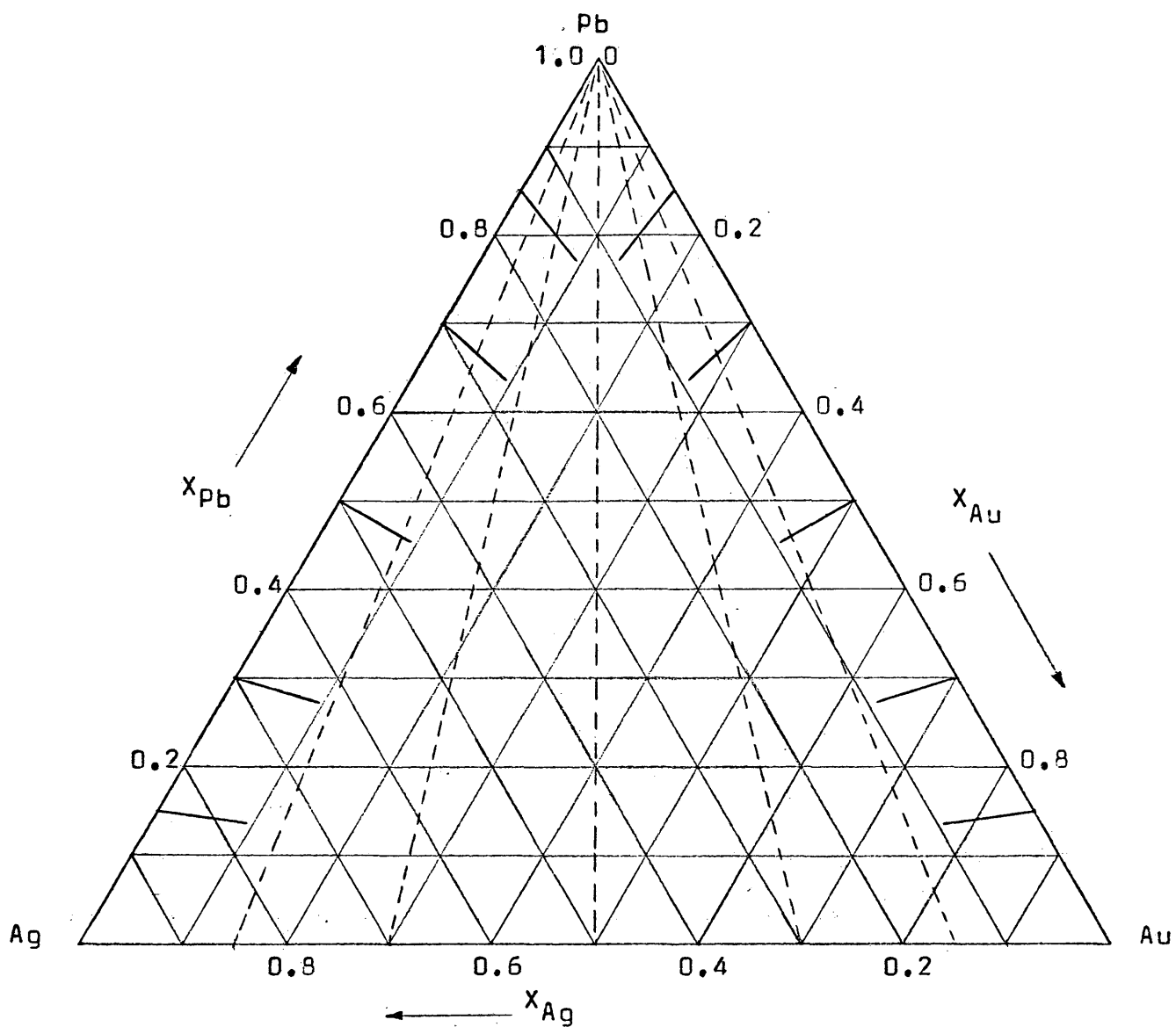


FIG. 17. PSEUDO-BINARIES SELECTED TO CALCULATE THE THERMODYNAMIC PROPERTIES OF THE Pb-Ag-Au SYSTEM.

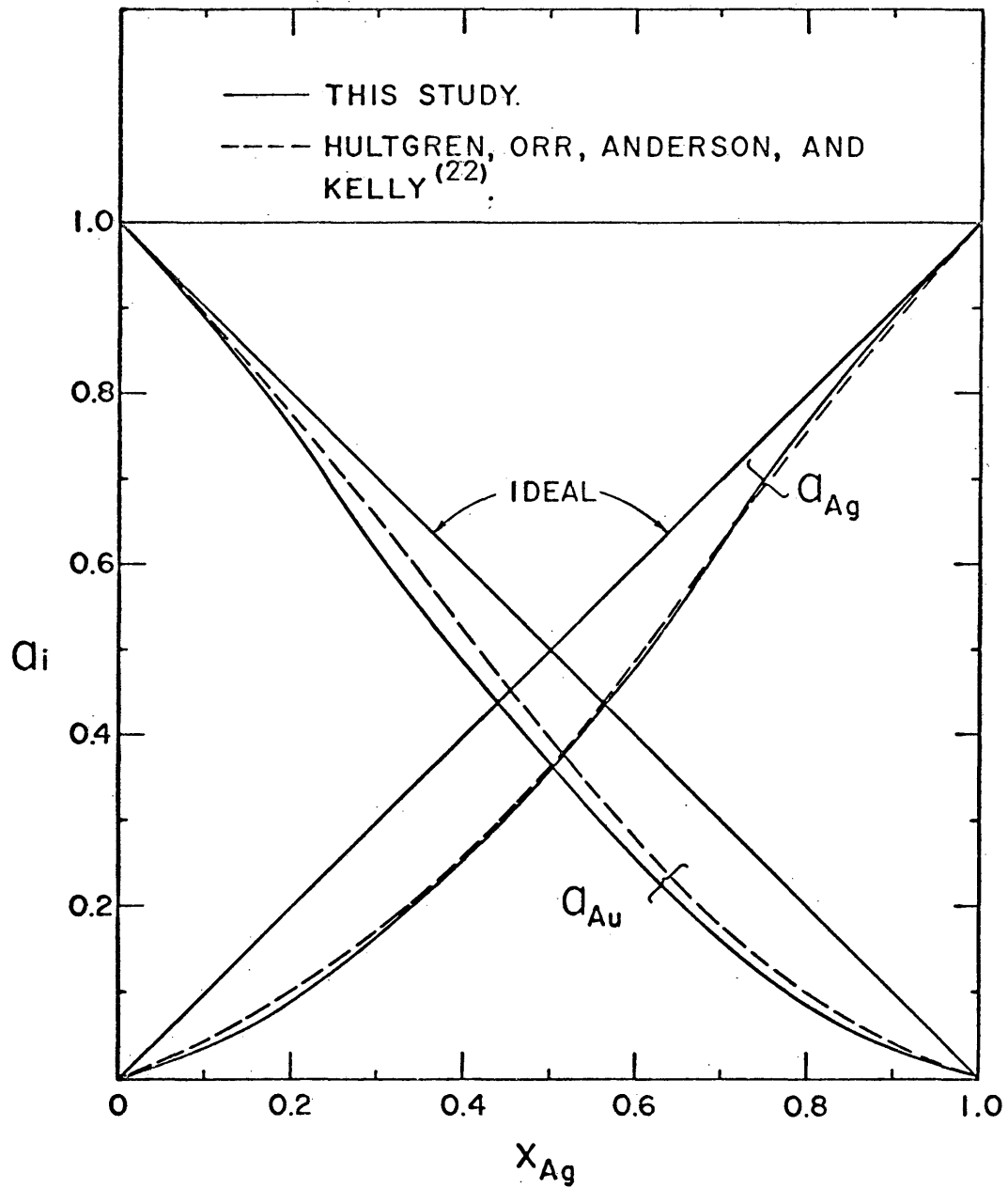


FIG. 18. ACTIVITIES OF SILVER AND GOLD IN THE LIQUID Ag-Au SYSTEM AT 1200° K.

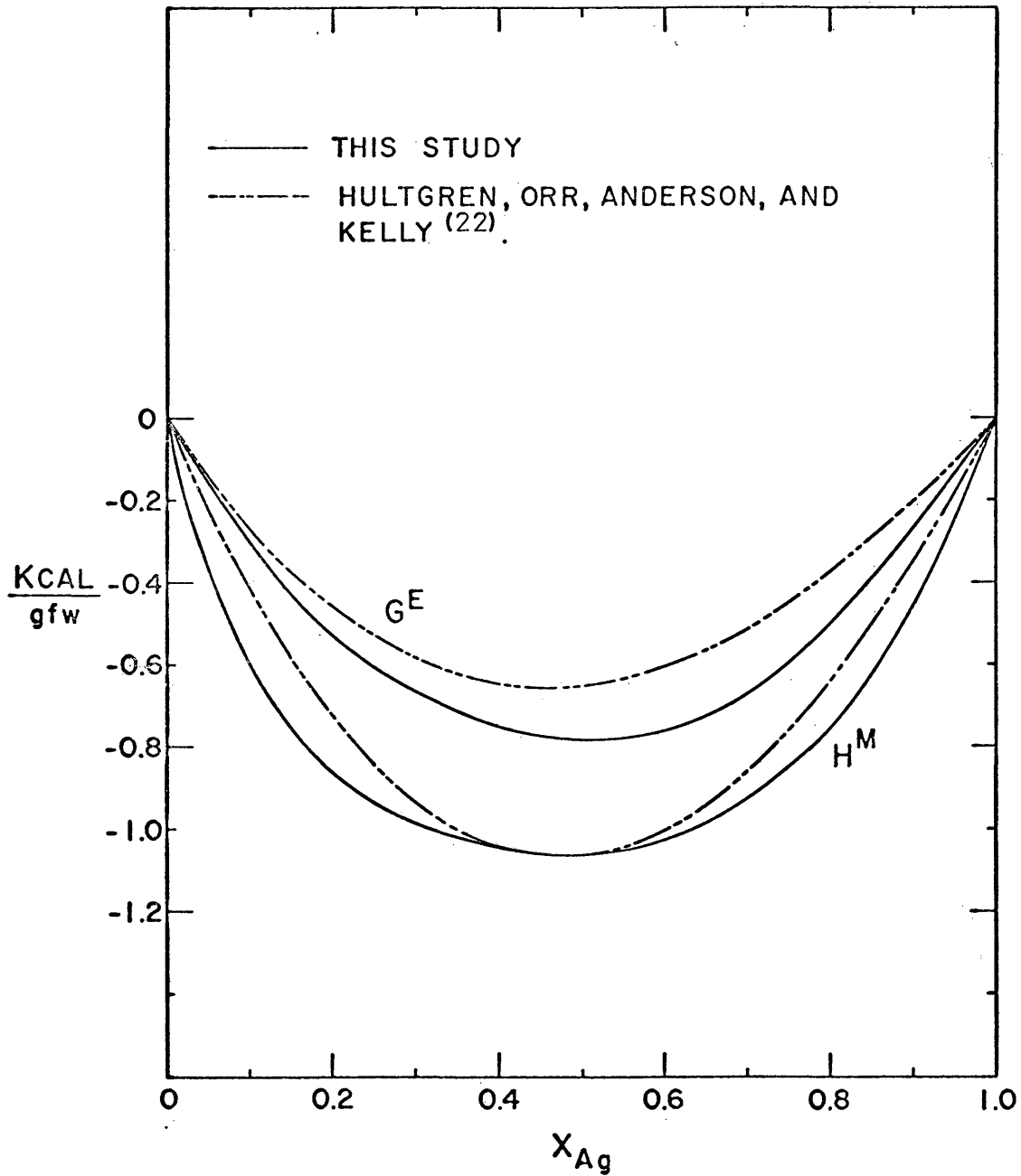


FIG. 19. EXCESS INTEGRAL MOLAR PROPERTIES OF THE LIQUID Ag-Au SYSTEM AT 1200° K.

B. Thermodynamic Data Compared to Current Solution Models.

There are three Solution Models which can be used to predict the thermodynamic behavior of certain systems. These models are:

- 1) Ideal Solution Model,
- 2) Regular Solution Model, and
- 3) Sub-Regular Solution Model.

1) An ideal solution fits the following conditions:

a) $H^M = 0$

b) $S^M = S^M(\text{ideal})$

c) $V^M = 0$

d) $\alpha_i = 0 \therefore a_i = X_i; i \rightarrow 1, 2, \dots, n$

2) A regular solution fits the following conditions:

a) $H^M \neq 0$

b) $S^M = S^M(\text{ideal})$

c) $\alpha_i = \text{constant}$

3) A sub-regular solution fits the following conditions:

a) $H^M \neq 0$

b) $S^M = S^M(\text{ideal})$

c) $\alpha_i = A + B \cdot X_i = \text{a linear function of composition.}$

For the systems Pb-Ag and Pb-Au, it has been found that none of the three current models can be applied. Furthermore, none of the five pseudo-binaries considered in this study meets the conditions of any of these solution models. However,

the results obtained for the silver-gold system indicate that this system fits reasonably well the Sub-Regular Solution Model as it is shown in Fig. 20.

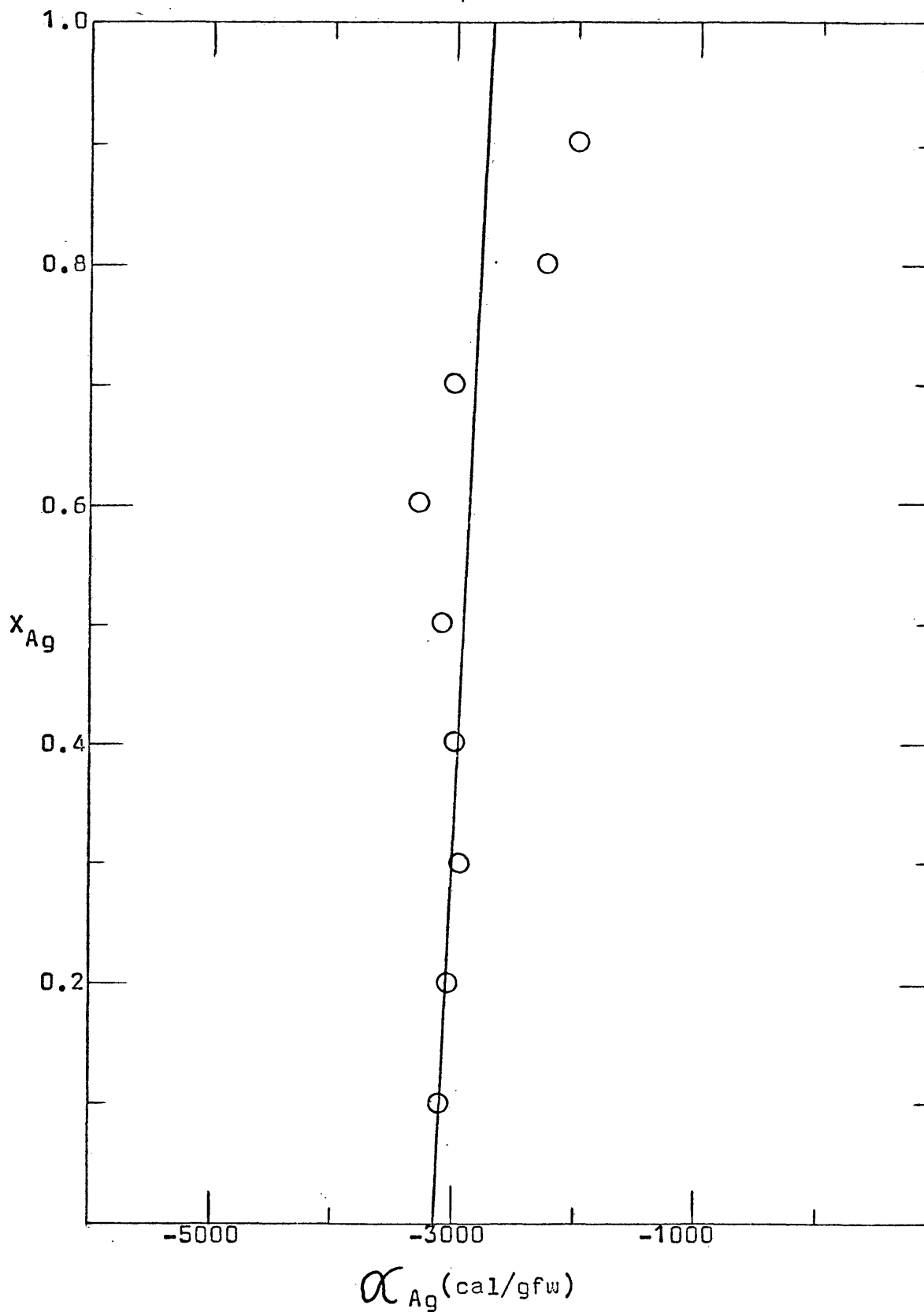


FIG. 20. ALPHA FUNCTION OF SILVER IN LIQUID Ag-Au ALLOYS AT 1200°K BY INTEGRATION FROM THE TERNARY FIELD.

VII. SUMMARY AND CONCLUSIONS

From the present study on the thermodynamic properties of the lead-silver-gold system, the following conclusions can be drawn:

1) There are no anomalies in the ternary field as it is indicated by the gradual change in the activities of each component in the ternary field.

2) The silver-gold system presents a consistently more negative Excess Integral Molar Free Energy of Mixing compared to previous works.

3) The molten oxide electrolyte appears to be a stable electrolyte even at very high temperatures.

4) The Ag-Au system fits reasonably well the Sub-Regular Solution Model.

5) The energy bond for the Pb-Ag-Au system seems to present a maximum at the stoichiometric ratio Pb_3AgAu_5 as it is indicated by the minimum on the G^E plot.

6) It is felt that the scatter in the experimental results is due mostly to the impossibility to get a perfect seal between the lead wire and its protective tube. The factor of 10 between the expansion coefficients of Mo and fused quartz easily destroys any seal as the temperature is raised.

VIII. SUGGESTIONS FOR FURTHER WORK.

Rather than undertaking an enumeration of the possible systems that can be studied using an electrolyte of the kind used in this study, it is felt that several critical points should be given as a guide to approach the best conditions to work on galvanic cell studies.

1) From this study and previous works^{4,5,14,15}, it is safe to say that any galvanic cell of the type used in this study should be feasible for operation, provided the thermodynamic condition of no displacement reaction is met, and that there are no side reactions present.

2) Since the reproducibility of the cell depends mainly on the degree of sealing between the lead wire and its protective tube, a pair of lead wires should not be used for more than one alloy composition. This practice will insure:

- a) A more random distribution of the experimental points,
- b) Better defined alpha and beta functions.

The lack of this requirement will produce activity curves defined as step functions. This is specially valid when working at temperatures higher than 800°C.

3) In any system, plots of dE/dT vs. X_i and E vs. X_i at

a given temperature should be made. From these plots corrected values of dE/dT and E may be taken to be used in the calculation of H^M and TS^M . This technique will decrease the possibility of getting H^M vs. X_i and TS^M vs. X_i plots with unusual shapes, specially at low and high mole fractions of i .

4) In a ternary system, each pseudo-binary should be done with a large number of points to provide enough information to define the alpha and the beta functions. At least 18 points are necessary since a large percentage of them do not count due to their high uncertainty.

5) The number of pseudo-binaries to be done in a ternary field depends on the characteristic of the system at hand. However, five pseudo-binaries seems to be reasonable.

6) In a ternary system the first pseudo-binaries to be worked out are those closer to the extreme binaries. These should give an idea whether or not the system at hand will require less than five pseudo-binaries. Generally, a drastic change in the e.m.f. compared to that for the extreme binaries indicates that a large number of pseudo-binaries must be worked out.

7) Alpha and beta functions should be drawn both along the pseudo-binaries themselves and as a function of "y" for constant X_i . This technique will provide a more reasonable way to defined the thermodynamic properties of the plain binaries.

8) A great deal of effort must be dedicated in trying to find a better way to make the contact between the lead wire and the electrode metal.

APPENDICES

APPENDIX A. Experimental Data for Liquid Pb-Ag Alloys.⁴

X_{Pb}	E, mv^{**}	$T(Liquidus)^*$
0.956	$- 3.90 + 0.64 \times 10^{-2} T$	-----
0.891	$- 3.61 + 0.96 \times 10^{-2} T$	-----
0.853	$- 2.88 + 1.12 \times 10^{-2} T$	-----
0.797	$- 1.45 + 1.30 \times 10^{-2} T$	-----
0.742	$- 4.89 + 1.91 \times 10^{-2} T$	-----
0.682	$- 4.21 + 2.13 \times 10^{-2} T$	-----
0.643	$- 7.53 + 2.75 \times 10^{-2} T$	-----
0.590	$-11.79 + 3.48 \times 10^{-2} T$	-----
0.522	$-11.23 + 3.72 \times 10^{-2} T$	-----
0.478	$-18.05 + 4.71 \times 10^{-2} T$	-----
0.445	$-17.60 + 4.98 \times 10^{-2} T$	-----
0.403	$-14.77 + 5.00 \times 10^{-2} T$	-----
0.361	$-19.84 + 5.85 \times 10^{-2} T$	-----
0.322	$-26.43 + 7.15 \times 10^{-2} T$	-----
0.293	$-24.38 + 7.35 \times 10^{-2} T$	-----
0.261	$-27.25 + 8.15 \times 10^{-2} T$	-----
0.182	$-25.23 + 9.88 \times 10^{-2} T$	773(772) ⁺
0.143	$-14.21 + 10.09 \times 10^{-2} T$	817(812) ⁺
0.096	$- 8.31 + 11.72 \times 10^{-2} T$	868(863) ⁺

* All temperatures in °C.

** Calculated by method of least squares. Equations represent values to within $\pm 0.5\%$ of actual experimental data.

+ Interpolated from the phase diagram.¹⁶

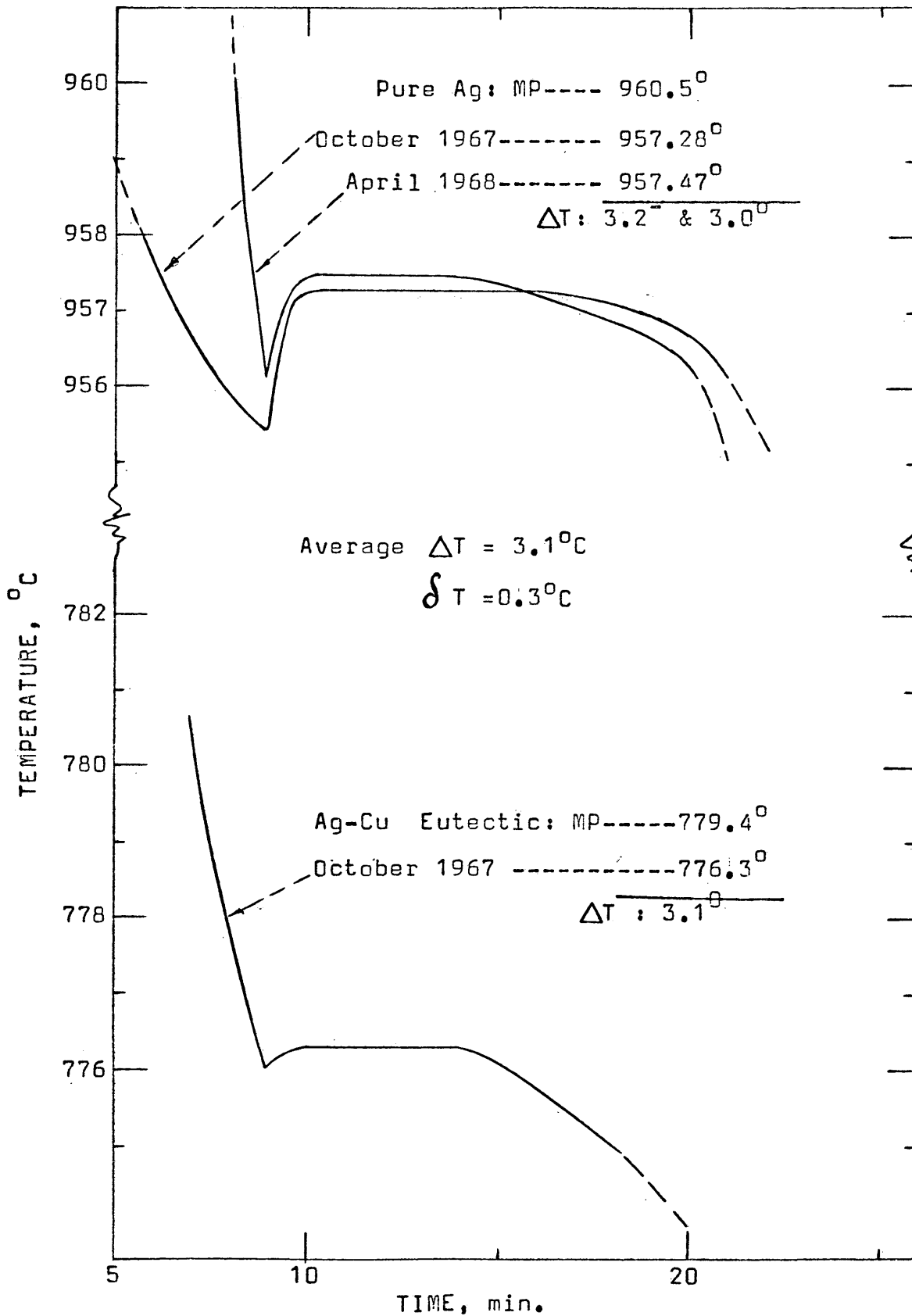
APPENDIX B. Experimental Data for Liquid Pb-Au Alloys.⁵

X_{Pb}	E, mv^{**}	$T(Liquidus)^*$
0.977	-3.11 + $4.56 \times 10^{-3} T$	----
0.939	-3.24 + $6.96 \times 10^{-3} T$	----
0.905	-1.99 + $8.48 \times 10^{-3} T$	----
0.882	-1.71 + $10.17 \times 10^{-3} T$	----
0.841	0.77 + $11.78 \times 10^{-3} T$	----
0.819	0.77 + $13.77 \times 10^{-3} T$	----
0.758	2.31 + $18.13 \times 10^{-3} T$	----
0.731	1.77 + $21.23 \times 10^{-3} T$	----
0.679	5.37 + $22.28 \times 10^{-3} T$	----
0.628	7.10 + $26.46 \times 10^{-3} T$	----
0.569	9.67 + $31.10 \times 10^{-3} T$	----
0.517	10.35 + $36.57 \times 10^{-3} T$	----
0.455	16.24 + $41.08 \times 10^{-3} T$	----
0.394	19.11 + $52.54 \times 10^{-3} T$	----
0.343	23.29 + $59.42 \times 10^{-3} T$	----
0.287	24.62 + $76.47 \times 10^{-3} T$	----
0.250	27.08 + $85.10 \times 10^{-3} T$	----
0.188	38.44 + $97.01 \times 10^{-3} T$	795
0.141	46.94 + $107.37 \times 10^{-3} T$	860
0.119	41.94 + $127.46 \times 10^{-3} T$	896
0.080	51.51 + $146.53 \times 10^{-3} T$	958
0.066	41.60 + $171.58 \times 10^{-3} T$	980
0.058	50.35 + $178.11 \times 10^{-3} T$	998
0.028	77.90 + $190.54 \times 10^{-3} T$	1032

* All temperatures in $^{\circ}C$.

** Calculated by method of least squares. Equations represent values to within $\pm 0.5\%$ of actual experimental data.

APPENDIX C. Calibration of Thermocouple.



APPENDIX D. Chemical Analysis of Materials.

1. Spectrographic Analysis of the lead, the silver,
and the gold.*

	<u>Lead</u>	<u>Silver</u>	<u>Gold</u>
Sb	N.D.	N.D.	N.D.
Tl	N.D.	N.D.	N.D.
Mg	2	2	1
Mn	N.D.	N.D.	N.D.
Pb	99.99 ⁺ %	1	3
Sn	N.D.	N.D.	N.D.
Si	N.D.	1	1
Cr	N.D.	N.D.	N.D.
Fe	1	2	1
Ni	N.D.	N.D.	N.D.
Bi	1	N.D.	N.D.
Al	N.D.	N.D.	N.D.
Ca	N.D.	N.D.	N.D.
Ag	N.D.	99.99%	2
Cu	3	20 ⁺	1
In	N.D.	N.D.	N.D.
Cd	N.D.	N.D.	N.D.
Zn	N.D.	N.D.	N.D.
Au	N.D.	N.D.	99.99 ⁺ %

* N.D.- None detected, and Impurities in ppm.

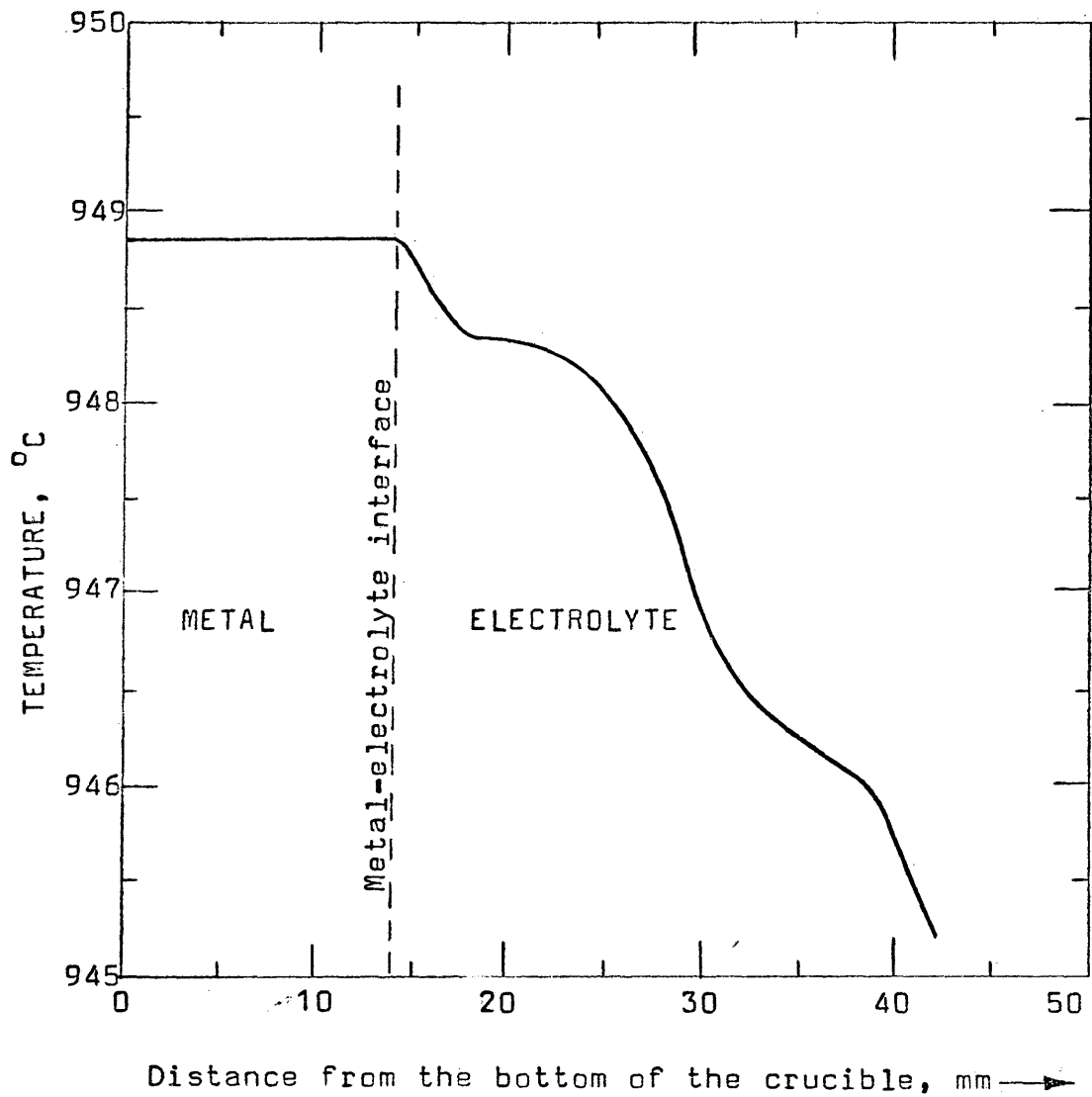
APPENDIX D. Chemical Analysis.....(continued)

2. Chemical Analysis of the Lead Oxide.

	<u>J.T. Baker</u>	<u>Mallincrodt</u>
Assay(PbO)	99.00 %	----
Insoluble in CH ₃ COOH	0.010 %	0.15 %
Chloride (Cl ⁻)	0.001 %	0.005 %
Nitrate (NO ₃ ⁻)	0.010 %	0.010 %
Silver(Ag)	0.0005 %	0.0001 %
Copper (Cu)	0.003 %	0.002 %
Iron (Fe)	0.0005 %	0.005 %
Not pp by H ₂ S(as SO ₄ ⁼)	0.02 %	0.20 %
Loss on Ignition	----	----

The SiO₂ used was 50/200 mesh silica for chromatographic columns. G. Frederick Smith Chemical Co.

APPENDIX E. Temperature profile of the metal and electrolyte inside the galvanic cell.



APPENDIX F. Atomic-Absorption Analysis of Lead and Gold
in Pb-Ag-Au Alloys.

The chemical analysis of all the alloys studied in the Pb-Ag-Au system was done with the Techtron Atomic-Absorption Spectrophotometer model AA-3.

By the atomic-absorption technique, the sample is first put into solution. The solution is vaporized in the appropriate flame where the element of interest is dissociated from its chemical bonds and placed into an unexcited, un-ionized "ground" state. Under these conditions, the element of interest absorbs radiation from a beam of light coming from a hollow cathode lamp made of the element being analyzed. The radiation absorbed is the same radiation the element would emit if it were excited.

The amount of energy absorbed by the element in the flame is a measure of its concentration in the solution from which it has been vaporized.

Up to a certain point of concentration, the plot Absorbance vs. Concentration is a straight line; therefore, with a series of standards of the element of interest a working curve is prepared from which the concentration of the element sought in any unknown can be read directly.

I. Experimental Procedure.

1) Known Samples. Three samples of weighed amounts of pure lead, pure silver, and pure gold were dissolved and analyzed to determine the accuracy to be obtained with the

APPENDIX F. Atomic-Absorption Analysis...(continued)

equipment used in this study.

2) Unknown Samples. Three samples of approximately 0.5 - 1.0 gram were used from each of the alloys studied.

II. Analytical Procedure.

The same analytical technique was used both for the knowns and for the unknowns. This technique is as follows:

1) Each alloy sample was first treated with HNO_3 , diluted to a convenient concentration, depending on the sample, to put into solution as much lead and silver as possible.

2) The solution and the remaining alloy from the preceding step were treated as follows:

a) The lead and silver nitrates in that solution were transformed into complex chlorides by a 4M sodium chloride solution.

b) The remaining alloy was dissolved in a minimum amount of aqua regia. The chlorides obtained were also transformed into complex chlorides by a 4M sodium chloride solution.

3) Solutions a) and b) were mixed together and diluted to one liter. Aliquots were diluted to be 3/4M in sodium chloride.

4) Separate sets of standards for lead and gold were prepared from 5 - 20ppm. Working curves for lead and gold were prepared for each set of 7 - 9 aliquots to be analyzed.

5) The three knowns were analyzed for lead and gold. Three aliquots were taken from each known. The same procedure was

APPENDIX F. Atomic-Absorption Analysis....(continued)

used for the unknowns.

6) In these analyses, the amount of silver present in each sample was obtained by difference since the high concentration of sodium chloride gave too much interference for silver both with the 3280.7- and 3382⁰Å lines.

7) From the analysis of the known samples, no interference between lead and gold was present.

III. Results.

The results for the chemical analysis of the three known samples are presented in Table 7, and those for the chemical analysis of the alloys studied are given in Table 8.

TABLE 7. Chemical Analysis of Knowns*

X_{Pb}	A	B	C	Average
0.4995	0.5025	0.4990	0.5010	0.5008
0.3075	0.3070	0.3067	0.3078	0.3072
0.1406	0.1406	0.1406	0.1400	0.1404

* Analyses in columns A, B, and C are averages of analyses of three aliquots.

APPENDIX F. Atomic-Absorption Analysis... (continued)

TABLE 8. — Chemical Analysis of Alloys.

$$R = X_{Ag}/X_{Au} = 5.627^{**}$$

A	B	C	Average X_{pb}
0.0912	0.0907	0.0999	0.094
0.2015	0.1952	0.1973	0.198
0.2951	0.2978	0.2972	0.297
0.3923	0.3961	0.3959	0.395
0.5032	0.4984	0.5000	0.501
0.6041	0.6068	0.5998	0.604
0.6980	0.6989	0.7035	0.700
0.7957	0.7993	0.8017	0.799
0.9157	0.9155	0.9142	0.915

** Obtained as an average of 81 analyses.

$$R = X_{Ag}/X_{Au} = 2.303^{**}$$

0.0997	0.1005	0.1001	0.100
0.2998	0.3000	0.2986	0.300
0.3960	0.3949	0.4004	0.397
0.5105	0.5141	0.5073	0.510
0.6088	0.6171	0.6127	0.613
0.6942	0.7079	0.6984	0.700
0.8095	0.8008	0.7998	0.803
0.9072	0.9062	0.9106	0.908

** Obtained as an average of 72 analyses.

APPENDIX F. Atomic-Absorption Analysis...(continued)

TABLE 8.— Chemical Analysis Of...(continued)

$$R = X_{Ag}/X_{Au} = 1.000^{**}$$

A	B	C	Average X_{pb}
0.1006	0.1000	0.1005	0.100
0.3003	0.3014	0.3038	0.302
0.4007	0.3985	0.3977	0.399
0.5034	0.4969	0.4963	0.499
0.6027	-----	0.5966	0.600
0.7035	0.6989	-----	0.701
0.7987	0.7982	0.7944	0.797
-----	0.9016	0.9011	0.901

** Obtained as an average of 63 analyses.

$$R = X_{Ag}/X_{Au} = 0.427^{**}$$

0.1030	0.0972	0.1001	0.100
0.3493	0.3520	0.3494	0.350
0.4011	0.4038	0.4019	0.402
0.4959	0.5071	0.5011	0.501
0.6015	0.5991	0.6027	0.601
0.6972	0.7035	0.6999	0.700
0.8022	0.8000	0.7911	0.798

** Obtained as an average of 63 analyses.

APPENDIX F. Atomic-Absorption Analysis...(continued)

TABLE 8. — Chemical Analysis of...(continued)

$$R = X_{Ag}/X_{Au} = 0.1765^{**}$$

A	B	C	Average X_{Pb}
0.0998	0.0998		0.100
0.2006	0.1991		0.200
0.3023	0.3014		0.302
0.3995	0.4011		0.401
0.4974	0.5010		0.500
0.6014	0.5992		0.600
0.7055	0.7053		0.705
0.8009	0.8032		0.802
0.8986	0.8989		0.899

** Obtained as an average of 54 analyses!

From tables 7 and 8, the maximum deviations are:

	<u>Standards</u>	<u>Alloys</u>
Maximum Deviation:	0.0015 X_{Pb}	0.008 X_{Pb}

APPENDIX G. Experimental Data for the Pb-Ag-Au System.

$$R = X_{Ag}/X_{Au} = 5.627$$

<u>T, °C</u>	<u>E, mv</u>	<u>T, °C</u>	<u>E, mv</u>	<u>T, °C</u>	<u>E, mv</u>
<u>X_{Pb} = 0.094</u>		<u>X_{Pb} = 0.198</u>		<u>X_{Pb} = 0.297</u>	
951.06	110.328	993.16	70.501	1030.86	54.946
893.60	101.511	945.80	65.858	975.33	49.956
831.06	66.277	892.33	59.117	929.65	46.045
768.19	41.793	833.04	53.696	867.65	41.612
796.26	52.122	793.20	49.503	809.61	37.012
847.11	75.193	760.48	38.698	788.30	35.246
866.71	85.395	860.50	56.334	837.42	39.293
914.20	104.802	903.29	61.195	903.72	44.114
968.92	114.934	957.75	66.871	1007.37	52.684
1018.57	120.507	1028.34	74.548		
<u>X_{Pb} = 0.395</u>		<u>X_{Pb} = 0.501</u>		<u>X_{Pb} = 0.604</u>	
1018.11	40.915	980.43	28.978	974.68	21.794
959.97	36.800	1035.55	31.214	1013.39	22.763
906.38	33.861	910.05	26.383	952.00	21.164
848.26	30.537	854.19	23.979	853.54	18.386
807.49	28.044	811.95	22.134	811.18	17.001
786.51	26.755	783.85	20.839	790.08	16.240
874.79	32.059	877.66	25.017	878.27	19.076
931.80	35.225	959.23	28.226	918.87	20.183
979.91	37.659				

APPENDIX G. Experimental Data for...(continued)

<u>T, °C</u>	<u>E, mv</u>	<u>T, °C</u>	<u>E, mv</u>	<u>T, °C</u>	<u>E, mv</u>
<u>X_{Pb}=0.700</u>		<u>X_{Pb}=0.799</u>		<u>X_{Pb}=0.915</u>	
1009.70	16.260	969.84	9.731	1025.07	4.635
957.64	15.448	909.20	9.169	981.30	4.384
908.96	14.803	847.33	8.445	924.00	4.202
850.19	13.672	804.70	7.869	870.29	4.001
811.49	12.877	784.19	7.553	831.10	3.900
782.68	12.354	872.34	8.531	784.54	3.714
864.11	13.768	937.77	9.231		
1023.27	16.458	1025.32	10.312		
975.83	15.480				

$$R = X_{Ag}/X_{Au} = 2.303$$

<u>X_{Pb}=0.100</u>		<u>X_{Pb}=0.300</u>		<u>X_{Pb}=0.397</u>	
1029.88	119.850	1028.07	51.980	1018.05	40.310
989.00	114.67	995.55	49.850	989.40	38.530
966.63	112.05	950.51	46.31	951.13	36.56
942.37	108.45	903.97	43.16	903.02	34.05
838.08	68.85	847.17	39.10	846.78	30.93
806.20	56.55	801.77	36.00	806.50	28.51
786.25	49.62	782.21	34.50	784.38	27.10
871.89	84.04	830.39	38.00	867.87	32.20
906.08	102.71				
928.83	107.20				

APPENDIX G. Experimental Data for... (continued)

$$R = X_{Ag}/X_{Au} = 2.303$$

<u>T, °C</u>	<u>E, mv</u>	<u>T, °C</u>	<u>E, mv</u>	<u>T, °C</u>	<u>E, mv</u>
<u>X_{Pb} = 0.510</u>		<u>X_{Pb} = 0.613</u>		<u>X_{Pb} = 0.700</u>	
974.40	29.21	1020.47	23.01	1024.98	17.50
946.14	28.18	987.54	22.02	981.58	16.50
904.32	26.62	951.73	20.88	950.92	15.87
846.03	24.33	902.82	19.53	904.64	14.96
804.76	22.49	846.64	17.91	849.24	13.77
781.52	21.33	804.13	16.49	806.95	12.74
862.21	25.08	781.65	15.90	790.00	12.27
1025.40	31.45	868.72	18.61	867.86	14.21
955.45	28.66	-----	-----	953.55	16.05
<u>X_{Pb} = 0.803</u>		<u>X_{Pb} = 0.908</u>			
1018.17	11.19	1023.33	5.51		
992.86	10.82	989.72	5.19		
957.09	10.42	955.58	4.87		
908.62	9.56	905.81	4.47		
845.72	8.66	855.59	4.00		
807.76	8.04	967.28	4.92		
789.72	7.70				
954.85	10.33				

APPENDIX G. Experimental Data for...(continued)

$$R = X_{Ag}/X_{Au} = 1.000$$

<u>T, °C</u>	<u>E, mv</u>	<u>T, °C</u>	<u>E, mv</u>	<u>T, °C</u>	<u>E, mv</u>
<u>X_{Pb}=0.100</u>		<u>X_{Pb}=0.302</u>		<u>X_{Pb}=0.399</u>	
1037.67	135.455	1030.79	67.306	993.54	49.006
999.88	128.103	979.08	63.802	953.20	47.154
960.59	123.493	938.08	60.813	901.55	44.454
912.95	111.746	881.24	56.754	844.74	40.634
854.48	85.996	806.68	51.356	807.29	38.605
814.84	72.515	782.81	49.794	779.84	37.155
785.36	63.691	853.17	54.854	824.56	39.617
880.99	98.003	902.94	58.022	876.92	42.288
				941.83	45.897
<u>X_{Pb}=0.499</u>		<u>X_{Pb}=0.600</u>		<u>X_{Pb}=0.701</u>	
968.25	32.554	1031.20	27.459	1023.83	18.790
914.01	30.523	916.98	24.062	957.89	18.226
847.18	27.857	963.39	25.065	902.61	17.277
809.92	26.096	1011.47	25.852	838.76	16.140
783.47	25.159	1024.12	26.159	810.61	15.669
835.27	27.512	940.47	24.511	785.14	15.010
877.43	29.047	848.75	22.052	870.94	17.118
1020.18	34.661	802.26	21.159	988.09	18.536
		776.03	20.197		
		880.03	23.011		

APPENDIX G. Experimental Data for... (continued)

$$R = X_{Ag}/X_{Au} = 1.000$$

<u>T, °C</u>	<u>E, mv</u>	<u>T, °C</u>	<u>E, mv</u>	<u>T, °C</u>	<u>E, mv</u>
<u>X_{Pb}=0.797</u>		<u>X_{Pb}=0.901</u>			
1032.08	12.166	1019.24	5.954		
985.310	11.788	981.35	5.752		
935.74	11.447	921.54	5.337		
872.95	10.865	852.99	5.125		
834.37	10.441	784.06	4.996		
784.868	9.780	829.38	5.076		
809.63	10.404	880.46	5.187		
917.62	11.522	953.00	5.480		

$$R = X_{Ag}/X_{Au} = 0.427$$

<u>X_{Pb}=0.100</u>		<u>X_{Pb}=0.350</u>		<u>X_{Pb}=0.402</u>	
1009.66	156.62	1036.07	69.74	1030.60	58.50
980.46	151.35	973.77	64.91	924.56	52.55
953.17	147.83	926.42	62.16	867.17	49.16
907.64	126.05	866.46	58.17	827.95	47.18
850.00	100.08	826.86	55.58	784.80	44.71
810.00	85.34	783.32	52.55	805.83	46.06
872.87	109.91	844.39	56.86	855.58	48.92
932.42	139.44	907.22	60.91	962.28	54.81
1036.85	158.85	948.00	63.48		

APPENDIX G. Experimental Data for ... (continued)

$$R = X_{Ag}/X_{Au} = 0.427$$

<u>T, °C</u>	<u>E, mv</u>	<u>T, °C</u>	<u>E, mv</u>	<u>T, °C</u>	<u>E, mv</u>
<u>X_{Pb} = 0.501</u>		<u>X_{Pb} = 0.601</u>		<u>X_{Pb} = 0.700</u>	
1031.24	42.14	1028.93	30.10	1028.52	20.05
967.63	39.75	999.69	29.45	1006.68	19.69
928.80	38.31	949.05	27.89	947.33	18.73
869.32	35.90	899.65	26.69	897.68	17.87
834.85	34.56	842.00	25.13	839.49	16.90
783.70	32.40	803.28	23.96	782.95	15.97
811.04	33.65	779.28	23.23	864.48	17.31
903.98	37.35	868.70	25.78	960.43	18.84
		921.02	27.24		

$$X_{Pb} = 0.798$$

1021.00	12.55
965.00	11.81
902.53	11.41
846.00	10.80
780.29	10.00
818.33	10.36
878.87	10.97
990.91	12.18

APPENDIX G. Experimental Data for...(continued)

$$R = X_{Ag}/X_{Au} = 0.1765$$

<u>T, °C</u>	<u>E, mv</u>	<u>T, °C</u>	<u>E, mv</u>	<u>T, °C</u>	<u>E, mv</u>
<u>X_{Pb}=0.100</u>		<u>X_{Pb}=0.200</u>		<u>X_{Pb}=0.302</u>	
1023.20	176.83	959.70	118.88	1030.37	92.71
978.40	169.97	915.65	114.64	976.25	88.20
932.98	155.20	852.37	108.27	933.62	85.09
874.11	125.74	810.34	98.21	873.20	80.35
837.87	109.42	791.75	92.13	837.22	77.41
790.94	92.17	877.41	110.95	784.36	72.91
825.06	104.72	935.62	116.82	805.34	74.87
901.55	143.63	994.40	122.24	883.15	81.27
957.81	168.11	1037.68	126.41		
995.94	173.24				
1034.32	178.35				
1010.10	175.10				
<u>X_{Pb}=0.401</u>		<u>X_{Pb}=0.500</u>		<u>X_{Pb}=0.600</u>	
846.34	55.58	1031.82	47.81	1033.25	32.88
806.98	52.83	966.25	45.05	975.58	31.57
780.20	51.02	902.90	42.35	935.60	30.11
867.40	56.98	849.85	40.22	875.16	28.94
1030.60	68.94	806.51	38.30	832.50	27.68
1002.85	66.58	787.07	37.38	782.06	25.90
955.62	64.04	874.09	41.32	846.54	28.13
		931.78	43.62	904.52	29.78
		998.38	46.20	988.87	32.07

APPENDIX G. Experimental Data for...(continued)

$$R = X_{Ag}/X_{Au} = 0.1765$$

<u>T, °C</u>	<u>E, mv</u>	<u>T, °C</u>	<u>E, mv</u>	<u>T, °C</u>	<u>E, mv</u>
<u>X_{Pb}=0.705</u>		<u>X_{Pb}=0.802</u>		<u>X_{Pb}=0.899</u>	
1031.96	21.64	1012.15	12.87	979.20	6.03
990.74	21.05	949.72	12.16	930.75	5.71
957.85	20.41	905.46	11.54	878.24	5.40
904.50	19.64	850.11	10.91	829.74	5.10
845.74	18.50	807.89	10.36	784.23	4.81
801.04	17.51	782.79	10.01	811.48	5.00
778.12	16.92	969.80	12.26	910.30	5.51
826.64	18.06	1030.88	13.06	1029.06	6.19
874.60	19.01				

LITERATURE CITED

1. N. W. Taylor: Jour. Am. Chem. Soc., 1923, vol. 45, p. 2895.
2. T. Chipman, J. F. Elliott, and B. L. Averbach: Experimental Equilibrium Methods at High Temperatures: the Physical-Chemistry of Metallic and Intermetallic Compounds, vol. 1, pp. 33-59, Chemical Publ. Co., 1960.
3. C. Wagner and A. Werner: J. of Electrochem. Soc., 1963, vol. 114, pp. 326-32.
4. J. P. Hager and I. A. Wilkomirsky: Trans. TMS-AIME, 1968, vol. 242, pp. 183-89.
5. J. P. Hager and R. A. Walker: Submitted to TMS-AIME.
6. K. A. Krakau and N. A. Vakhramer: Keram. i Steklo, 1932, vol. 8, p. 42.
7. R. F. Geller, A. S. Creamer, and E. N. Bunting: J. Res. Nat. Bur. Standards, 1934, vol. 13, p. 237.
8. K. A. Krakau, E. J. Mukhin, and M. S. Heinrich: C. R. Acad. Sci. U.S.S.R., 1937, vol. 14, p. 281.
9. E. Preston and W. E. S. Turner: J. Soc. Glass Tech., 1935, vol. 14, p. 296.

10. R. T. Callow: Trans. Faraday Soc., 1951, vol. 47, p. 370.
11. L. Shartis and E. S. Newman: J. Res. Nat. Bur. Standards, 1948, vol. 40, p. 471.
12. F. D. Richardson and L. E. Webb: Trans. Instn. Mining and Metallurgy, 1955, vol. 64, pp. 529-64.
13. H. Ito and T. Yanegese: Trans. Japan Inst. Metals, 1962, vol. 56, p. 2931.
14. T. O'MBockris and J. A. Kitchener: J. Phys. Chem., 1952, vol. 54, pp. 536-48.
15. T. O'MBockris and G. W. Mellors: J. Phys. Chem., 1956, vol. 60, pp. 1321-28.
16. M. Hansen: Constitution of Binary Alloys, 2nd ed., pp. (40, 222, 5), McGraw-Hill Book Co., New York, 1958.
17. M. Kawakami: Sci. Repts. Tohoku Imp. Univ., 1930, vol. 19 pp. 521-49.
18. H. O. Von Samson-Himmelstjerna: Z. Metallk., 1936, vol. 28, pp. 197-202.
19. O. T. Kleppa: J. Phys. Chem., 1956, vol. 60, pp. (446, 452, 440).
20. R. L. Orr and P. H. Sommelet: Gibbs Energies, Entropies and Heats of Formation from Drop-Calorimetry: the Lead-Silver System, pp. 24-38, Univ. of Calif., Berkely, 1965.

21. A. A. Granovskaya and A. P. Liubimov: Zhur. Fiz. Khim., 1953, vol. 27, pp. 1437-45.
22. R. Hultgren, R. L. Orr, P. D. Anderson, and K. K. Kelley: Selected Values of Thermodynamic Properties of Metals and Alloys, pp. (377, 484, 340), John Wiley and Sons, New York, 1963.
23. A. T. Aldred and J. N. Pratt: Trans. Faraday Soc., 1961, vol. 57, pp. 611-18.
24. J. Terpilowski: Arch. Hutnictwa, 1957, vol. 2, pp. 289-304.
25. V. N. Eremenko: Ukrain. Khim. Zhur., 1957, vol. 23, pp. 6-12.
26. D. Kubaschewski and C. M. Catterall: Thermochemical Data of Alloys, p. 86, Pergamon Press, New York, 1956.
27. R. Vogel: Z. anorg. Chem., 1905, vol. 45, pp. 11-23.
28. D. Kubaschewski: Z. Phys. Chem., 1943, vol. 192, p. 292.
29. D. J. Kleppa: J. Am. Chem. Soc., 1949, vol. 71, pp. 3275-80.
30. E. Janecke: Metallurgie, 1911, vol. 8, pp. 599-600.
31. U. Raydt: Z. anorg. Chem., 1912, vol. 75, pp. 58-62.
32. C. Wagner: Acta Met., 1954, vol. 2, pp. 242-49.
33. C. Wagner and G. Engelhardt: Z. Physik Chem., 1932, vol. 159, pp. 241-67.
34. R. A. Oriani: Acta Met., 1956, vol. 4, pp. 15-24.

35. L. S. Darken: J. Am. Chem. Soc., 1950, vol. 72,
pp. 2909-14.
36. C. Wagner: Thermodynamic of Alloys, 2nd ed., pp. 19-22,
Addison-Wesley Publ. Co., Reading, 1962.
37. J. Topping: Errors of Observation and Their Treatment,
3rd ed., pp. 16-24, Chapman and Hall Ltd., London,
1966.

BIOGRAPHICAL NOTE

The author was born in Mompos, Colombia, South America, on September 27, 1934. He received his primary and secondary education in Mompos.

In February 1957 he attended the Universidad Nacional de Colombia, Facultad de Minas, Medellin, and received his Mines and Metallurgical Engineering degree in 1961.

In 1962 he began to work for the Universidad Nacional de Colombia as an assistant professor. In June 1966, the Universidad Nacional de Colombia and the Ministerio de Minas de Colombia granted him economical support to pursue a Master of Science Degree in Metallurgical Engineering.

He is married to the former Leonor Serrano-Camacho, from Mompos.